Towards critical low-temperature relaxation indicators for effective rejuvenation efficiency evaluation of rejuvenator-aged bitumen blends

Ren, Shisong; Liu, Xueyan; Erkens, Sandra

DOI
10.1016/j.jclepro.2023.139092

Publication date
2023

Document Version
Final published version

Published in
Journal of Cleaner Production

Citation (APA)
Ren, S., Liu, X., & Erkens, S. (2023). Towards critical low-temperature relaxation indicators for effective rejuvenation efficiency evaluation of rejuvenator-aged bitumen blends. *Journal of Cleaner Production*, *426*, Article 139092. https://doi.org/10.1016/j.jclepro.2023.139092

Journal of Cleaner Production 426 (2023) 139092

Contents lists available at ScienceDirect

Journal of Cleaner Production

journal homepage: www.elsevier.com/locate/jclepro

Towards critical low-temperature relaxation indicators for effective rejuvenation efficiency evaluation of rejuvenator-aged bitumen blends

Shisong Ren *, Xueyan Liu, Sandra Erkens

Section of Pavement Engineering, Faculty of Civil Engineering and Geosciences, Delft University of Technology, the Netherlands

ARTICLE INFO

Handling Editor: Zhen Leng

Keywords:
Critical relaxation indicator
Rejuvenator type/dosage
Aging degree
Free volume ratio
Molecular mobility
Molecular dynamics simulation

ABSTRACT

The relaxation behavior affected by aging and rejuvenation plays a crucial role in its low-temperature cracking potential of bitumen. However, there are limited studies on the relaxation performance of rejuvenated bitumen under different rejuvenation conditions. This paper aims to propose critical indicators to assess the rejuvenation efficiency of low-temperature relaxation performance of various rejuvenated binders. The effects of rejuvenator type/dosage and aging level on relaxation parameters are investigated. The τ_{50s}, $t_{25\%}$, and A are recommended as critical indicators based on their high sensitivities to influence factors and rejuvenation percentage scope. Additionally, molecular dynamic simulation outputs on virgin/aged bitumen and rejuvenators explain the difference in rejuvenation effectiveness of different rejuvenators. The results show that bio-oil rejuvenator exhibits the highest efficiency on regenerating the relaxation performance. All relaxation parameters of aged bitumen can be regenerated by adding rejuvenators. MD simulations reveal that the molecular mobility and free volume ratio of rejuvenators mainly cause the difference in rejuvenation efficiency on the relaxation property between various rejuvenators. The diffusion capacity of rejuvenator shows a more dominant effect on rejuvenation efficiency than fractional free volume.

1. Introduction

The principles of circular economy and sustainable development are increasingly influencing pavement research (Schwettmann et al., 2023; Mokhtari et al., 2017). Current studies focus on maximizing the reuse of waste reclaimed asphalt pavement (RAP) materials while maintaining the mechanical performance of asphalt pavement across the entire temperature spectrum (Shi et al., 2022; Fang et al., 2021; Ahmed and Hossain, 2020). Recycled asphalt mixtures offer significant and undeniable cost-saving and environmentally-friendly benefits, as shown by life cycle analysis (Yan et al., 2021; Ren et al., 2021a,b). However, the primary challenge with RAP is the inadequate low-temperature cracking resistance of asphalt materials due to the high stiffness of aging bitumen, which impairs relaxation performance and raises the risk of thermal cracking at low-temperatures (Jing et al., 2021; Gulzar et al., 2023).

Several rejuvenators have been developed and utilized to enhance the low-temperature properties of aged bitumen in RAP materials (Behnood, 2019; Rajib et al., 2022; Li et al., 2022). These rejuvenators comprise lightweight molecules designed to disperse asphaltene clusters, rebalance chemical components (colloidal structures), and improve the low-temperature behavior of aged bitumen (Zhao et al., 2018; C. Liu et al., 2022). However, the effectiveness of rejuvenation depends on various factors, including the type of rejuvenator, rejuvenator dosage, bitumen aging level, RAP binder dosage, among others (Zeng et al., 2022; Bai, 2017; Wang et al., 2023). Moreover, diverse evaluation indicators significantly affect the rejuvenation percentages of rejuvenator-aged bitumen blends (Xu et al., 2021a,b; D. Wang et al., 2021) due to the random selection methods.

Various rheological and chemo-physical properties have been utilized to quantitatively assess the impact of material factors (aging, rejuvenation, and modification) and testing conditions (temperature) on the low-temperature performance of bituminous materials. A summary of low-temperature rheological evaluation parameters is presented in Table 1. The bending beam rheometer (BBR) test is the most commonly used method of estimating the low-temperature cracking potential of bitumen based on stiffness (S), m-value, ΔT_c, $T_{s\,=\,300}$, and $T_{m\,=\,0.3}$ parameters. Other rheological tests include Fraass breaking point, single edge notched beam (SENB), asphalt binder cracking device (ABCD), cone penetration (CPT), and ductility tests. Additionally, chemo-physical methods, such as SARA fractionation, Fourier-transform

* Corresponding author.
E-mail address: Shisong.Ren@tudelft.nl (S. Ren).

https://doi.org/10.1016/j.jclepro.2023.139092
Received 17 April 2023; Received in revised form 31 July 2023; Accepted 28 September 2023
Available online 29 September 2023

infrared (FTIR) spectroscopy, differential scanning calorimetry (DSC), and atomic force microscopy (AFM) were used to explain the reasons for difference in low-temperature properties (Hofer et al., 2023). It was reported that FTIR spectroscopy and SARA fractionation provided information regarding low-temperature behavior of bitumen. Furthermore, the glass transition temperature Tg was closely related to low-temperature rheological parameters (T. Wang et al., 2021; Lin et al., 2021; Zhang et al., 2015; Kumbargeri et al., 2023). However, there is no general guideline on selecting testing methods and evaluation indices for determining the low-temperature performance of bitumen.

The relaxation performance of bitumen measured from DSR tests was highly correlated with its low-temperature cracking resistance from stress accumulation, as noted by Jing et al. (2020). Buchner et al. (2023a,b) argued that the BBR test could not comprehensively estimating the low-temperature property of bitumen since it was a creep test and not a relaxation test. The relaxation behaviors of bitumen and mastic were characterized to analyze the effects of aging and rejuvenation on their cracking resistance. Regarding the rejuvenation efficiency, it was essential to consider the low-temperature relaxation behaviors of rejuvenated bitumen (Zhang and Greenfield, 2007). However, numerous variations in material characteristics, such as rejuvenator type/dosage and aging degree of bitumen, and relaxation parameters (i.e., shear stress, relaxation time, residue stress), considerably hindered to develop evaluation method for rejuvenation efficiency (Sonibare et al., 2021; Sun and Wang, 2022; Yaphary et al., 2022). The reason for the difference in rejuvenation efficiency in different rejuvenator-aged bitumen systems is still vague, despite diverse randomized studies being conducted. (Xu et al., 2021a,b; Luo et al., 2023; S. Liu et al., 2022).

The objectives of this study can be summarized as follows: (1) systematically investigating the intricate influence of rejuvenator type/dosage and aging level of bitumen on the low-temperature relaxation behaviors of rejuvenated bitumen; (2) proposing preliminary decisive relaxation indices to evaluate the rejuvenation effectiveness of a broad range of rejuvenators regarding low-temperature performance; and (3) explaining underlying mechanism on the difference in rejuvenation efficiency of various rejuvenators at an atomic level.

The research structure adopted in this study is depicted in Fig. 1. Initially, different rejuvenated binders were fabricated by using variant rejuvenator types (BO, EO, NO, and AO) and the degree of bitumen aging (LAB20, LAB40, and LAB80). Subsequently, the relaxation tests were conducted on virgin, aged, and rejuvenated binders to assess the impact of aging and rejuvenation on the relaxation performance of bitumen with variable relaxation parameters and corresponding rejuvenation percentages. Moreover, a relaxation model was applied to relaxation curves and the model parameters were estimated to represent potential evaluators of rejuvenation efficiency. Finally, the molecular dynamics simulation technique was employed to predict and compare the volumetric, thermal, and dynamic parameters of aged binders and different rejuvenators to unravel the fundamental mechanism behind the difference in relaxation performance of various rejuvenated binders.

2. Materials and experimental methods

2.1. Materials

The raw materials involved in this study contain virgin bitumen and rejuvenators. The 70/100 virgin bitumen was utilized with its physicochemical properties listed in Table 2. Based on the rejuvenator classification (Ncat, 2014), four rejuvenators (bio-oil, engine-oil, naphthenic-oil, and aromatic-oil) are adopted. Table 3 displays the physical indices, average molecular weight, and element components of rejuvenators.

2.2. Preparation of aged and rejuvenated binders

The 70/100 bitumen was used to artificially fabricate the aged bitumen using the Thin Film Oven test (TFOT) and Pressure Aging Vessel (PAV) for simulating short-term and long-term aging. For all aged binders, the temperature and aging time of FTOT were 163 °C and 5 h. The aging temperature of PAV was 100 °C, while the aging time varied from 20 to 40 and 80 h for preparing the aged bitumen with different

Table 1
Low-temperature performance evaluation of bituminous materials.

	Rheological tests	Rheological indicators	Influence factors	Chemo-physical tests	Ref
1	BBR, 4 mm DSR	S, m-value; ΔTc G[a], δ	Temperature; Bitumen type	ATR-FTIR, SARA fractionation	Hofer et al. (2023)
2	BBR, Fraass breaking point	S, m, $T_{s=300}$, $T_{m=0.3}$, Fraass breaking point;	RAP binder dosage; rejuvenator; polybutadiene rubber	SARA fractionation; DSC	Mansourkhaki et al. (2020)
3	BBR	S, m-value	SARA ratio	SARA and DSC fractionation	Wang et al. (2021)
4	DSR relaxation	G-R, residue stress	Rejuvenator type/dosage	DSC	Lin et al. (2021)
5	BBR, Single Edge Notched Beam	S, m-value, fracture load, fraction deflection, fracture toughness, fracture energy	Bio-based and refined waste oil content	DSC	Zhang et al. (2015)
6	BBR, Asphalt binder cracking device (ABCD)	$T_{s=300}$, $T_{m=0.3}$, ΔT_c, ΔT_f	Binder source, compositional chemistry, crude oil processing, modification type, thermal properties	SARA, DSC	Kumbargeri et al. (2023)
7	Ex-BBR, cone penetration test (CPT)	Critical grading temperature, cone penetration depth	Different modifiers, reversible aging level	Atomic force microscopy (AFM)	Ren et al. (2022)
8	DSR relaxation, BBR	Shear stress, percentual stress relaxation at 30min and 60min, m-value	Bitumen type, temperature,	–	Buchner et al. (2023)
9	DSR relaxation	Shear stress, residue stress, relaxation time	Aging time, temperature, and pressure	–	Jing et al. (2020)
10	Ductility, Creep, and relaxation test	Shear stress	Layer double hydroxides (LDHs)/crumb rubber modified bitumen and UV aging level	FTIR	Pang et al. (2014)
11	DSR relaxation, BBR, SENB	Shear stress, stress ratio, relaxation time, S, m-value, fracture energy, maximum fracture displacement	Asphalt binder and mastic type	DSC	Zheng et al. (2022)
12	DSR relaxation	Shear stress, residue stress, relaxation model parameters	limestone particle size	–	Xing et al. (2020)
13	DSR Relaxation	Percentage stress relaxation after 60min	Rejuvenator type, dosage,	–	Buchner et al. (2023)

[a] BBR: Beam Bending Rheometer; SARA: Saturate (S), Aromatic (A), Resin (R), Asphaltene (As); DSR: Dynamic Shear Rheometer; S: Stiffness; FTIR: Fourier Transform Infrared Spectroscopy; DSC: Differential Scanning Calorimetry.

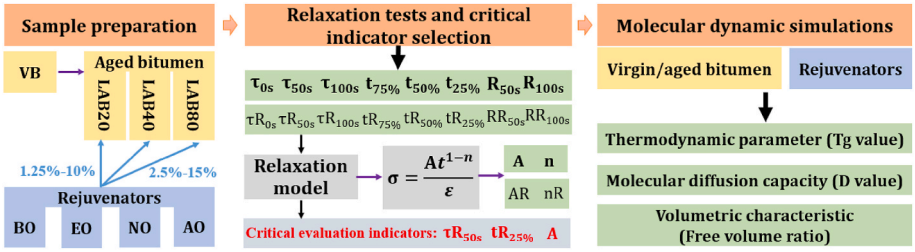

Fig. 1. Flow chart of the main structure and methodology in this study.

Table 2
The basic properties of virgin bitumen.

Properties	Value	Specification
25 °C Density (g·cm^{-3})	1.017	EN 15326
25 °C Penetration (0.1 mm)	91	ASTM D35
Softening point (°C)	48.0	ASTM D36
135 °C Viscosity (Pa·s)	0.80	AASHTO T316
Saturate dosage (wt%)	3.6	ASTM D4124
Aromatic dosage (wt%)	53.3	
Resin dosage (wt%)	30.3	
Asphaltene dosage (wt%)	12.8	

Table 3
Chemical and physical indices of rejuvenators.

Properties	Bio-oil	Engine-oil	Naphthenic-oil	Aromatic-oil
25 °C Density (g·cm^{-3})	0.911	0.833	0.875	0.994
25 °C Viscosity (cP)	50	60	130	63100
Flash point (°C)	265–305	>225	>230	>210
Average weight Mn (g·mol^{-1})	286.43	316.48	357.06	409.99
Carbon dosage (wt%)	76.47	85.16	86.24	88.01
Hydrogen dosage (wt%)	11.96	14.36	13.62	10.56
Sulfur dosage (wt%)	0.06	0.13	0.10	0.48
Oxygen dosage (wt%)	11.36	0.12	0.10	0.40
Nitrogen dosage (wt%)	0.15	0.23	0.12	0.55

long-term aging degrees. The virgin and various aging bitumen were abbreviated as VB, LAB20, LAB40, and LAB80.

The material components in different rejuvenated binders are summarized in Fig. 2. Twelve groups of rejuvenated bitumen were manufactured with three aging levels and four rejuvenators. The aged bitumen was preheated and mixed with rejuvenators at 160 °C for 10 min to ensure homogeneous dispersion of the rejuvenator. Considering the slight aging level, the rejuvenator dosages in LAB20 varied from 1.25% to 10%. To the severely-aged bitumen (LAB40 and LAB80), the rejuvenator concentration changed from 2.5% to 15% with an interval of 2.5%. In total, 72 kinds of rejuvenated binders were fabricated for relaxation behavior characterization, considering effects of rejuvenator type/dosage and aging grade of bitumen.

2.3. Relaxation test

The relaxation test was performed with a dynamic shear rheometer (DSR) at 0, 10, and 20 °C. The geometry of the parallel plate was set as 2 mm in thickness and 8 mm in diameter. Moreover, the relaxation test was conducted with a strain-control model (a fixed strain of 1%). As shown in Fig. 3, two steps were included in the relaxation procedure: increasing-strain loading (0–0.1s) and constant-strain loading (0.1–100s). The strain rose from 0% to 1% during the first step, which was 1% in a relaxation time of 100s. The residue shear stress τ, relaxation time t, and shear stress ratio R were used to evaluate the relaxation performance of bituminous materials. However, it should be mentioned that these relaxation parameters varied at different relaxation stages. Therefore, three residue shear stress at 0s, 50s, and 100s (τ_{0s}, τ_{50s}, τ_{100s}), three relaxation time with 75%, 50%, and 25% stress reduction ($t_{75\%}$, $t_{50\%}$, $t_{25\%}$), and stress ratio at 50s and 100s (R_{50s}, R_{100s}) were selected to evaluate the rejuvenation efficiency of various rejuvenator-aged bitumen blends systematically.

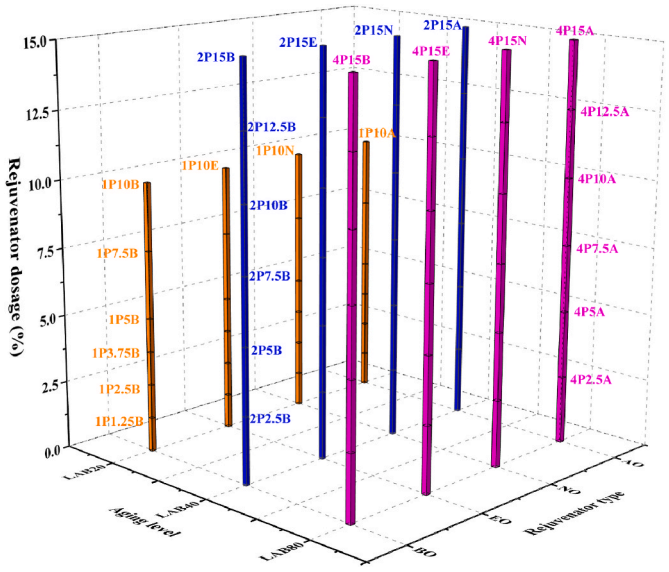

Fig. 2. Sample summarization of this study.

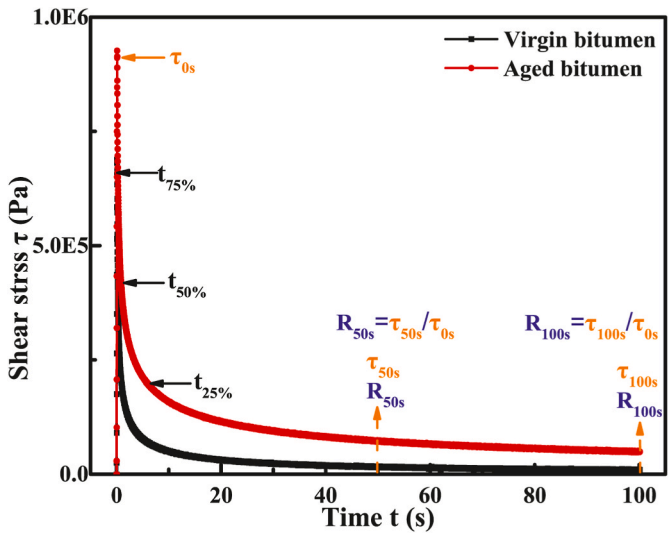

Fig. 3. The representative relaxation curves of virgin and aged bitumen.

2.4. Differential scanning calorimetry (DSC) test

It is recognized that the glass transition temperature Tg is significantly associated with the low-temperature relaxation and cracking potential of polymer and bituminous materials. This study implemented DSC tests (manufactured by PerkinElmer company) to measure the Tg values of virgin/aged bitumen and rejuvenators. About 10 mg bitumen or rejuvenator sample was encased in an aluminium plate in a sample room. The testing temperature increased from room temperature to 160 °C with an increment rate of 20 °C/min to completely relax the bitumen or rejuvenator molecules. Afterward, the testing temperature declined gradually to −70 °C at 10 °C/min to determine the Tg point based on the heat flow-temperature curve.

3. Experimental results and discussion

3.1. Long-term aging effect on relaxation performance

The aging effect on the relaxation behaviors of bitumen is reflected with shear stress τ, relaxation time t, and stress ratio R parameters. The corresponding results are displayed in Fig. 4. As the long-term aging time prolongs, the Log(τ) and Log(t) values of bitumen increase linearly, while the R parameter at 0 and 10 °C enlarges exponentially. Additionally, the influence level of long-term aging on the relaxation behavior of bitumen depends on the evaluation index type and testing temperature based on the difference in correlation equations. As the temperature and relaxation time rising, the slope and intercept values in Log(τ)-t equations enlarge and reduce, respectively. It implies that aging degree shows a greater effect on the shear stress of bitumen at high temperatures and long relaxation time, resulting in a lower τ value. Meanwhile, the relaxation time influence is more significant than temperature variation.

The severe aging level leads to an obvious increment in relaxation time t, rising as residue stress ratio declines from 75% to 25% but tending to decrease as the temperature grows. A high temperature would promote the enlargement in molecular mobility and reduction in intermolecular interactions between bitumen molecules, and thus a shorter relaxation time is required for molecular relaxation. The low residue stress ratio increases the slope value, which drops as the temperature rises. Moreover, the influence of reside stress ratio on the sensitivity of relaxation time to long-term aging time is greater than the temperature. Similar to the τ parameter, the long relaxation time and high temperature result in a low R value of bitumen. As the relaxation time and temperature increase, the R value and its sensitivity to long-term aging time reduce gradually. When the temperature is 20 °C, there is no clear relationship between the R value of bitumen and aging time.

3.2. Rejuvenation influence on relaxation parameters of aged bitumen

3.2.1. Shear stress τ

The shear stress τ parameters at 0s, 50s, and 100s of LAB40 rejuvenated bitumen are shown in Fig. 5. All τ values of rejuvenated bitumen exhibit a linear decreasing trend as the rejuvenator dosage increases. The addition of rejuvenators significantly reduces the stiffness and shear stress of aged bitumen. These four rejuvenators have different restoration effects on the τ value of aged bitumen. Based on the absolute scope values of correlation equations, bio-oil rejuvenator maximally restores the τ value, followed by engine-oil and naphthenic-oil, while aromatic-oil rejuvenated bitumen has the highest τ parameter. Additionally, the

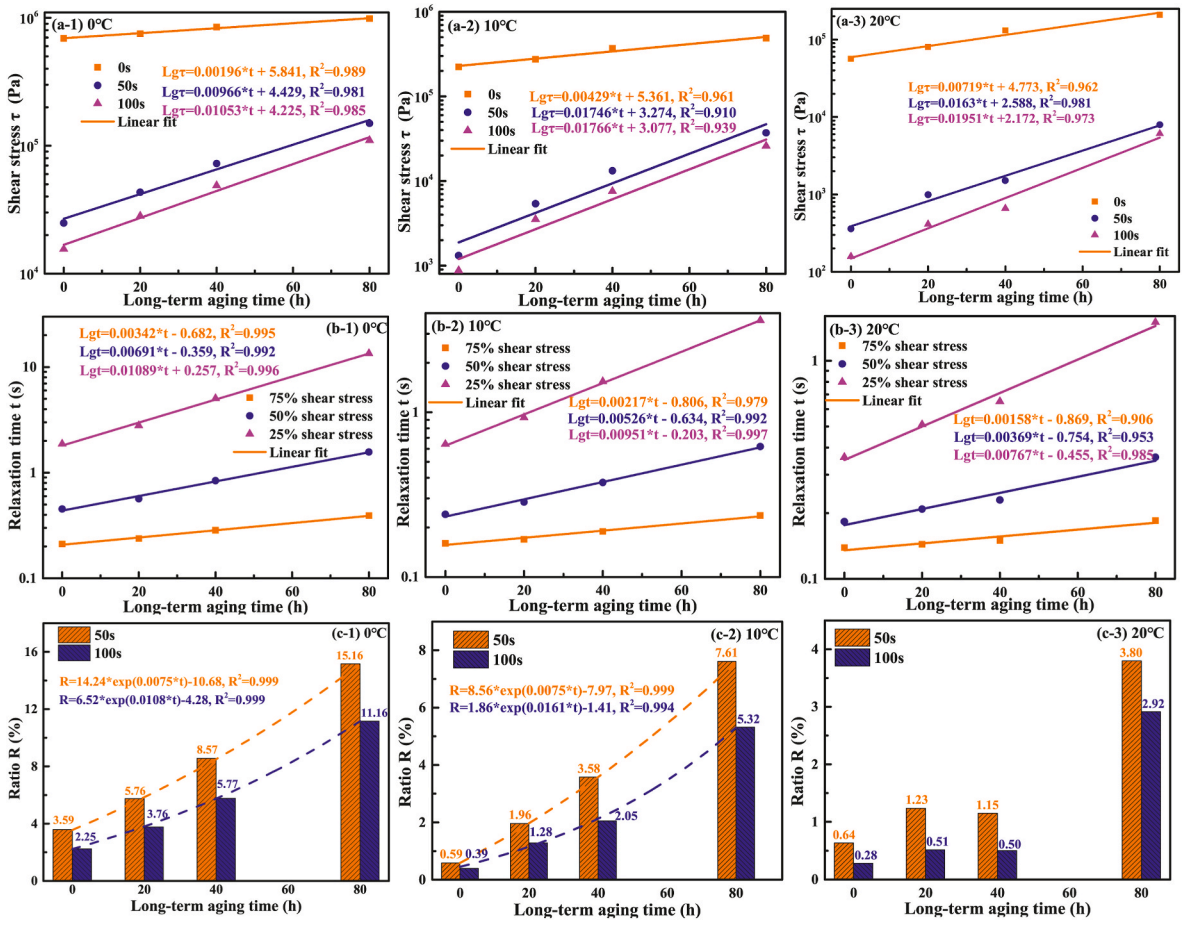

Fig. 4. Relaxation parameters of virgin and aged bitumen at different temperatures.

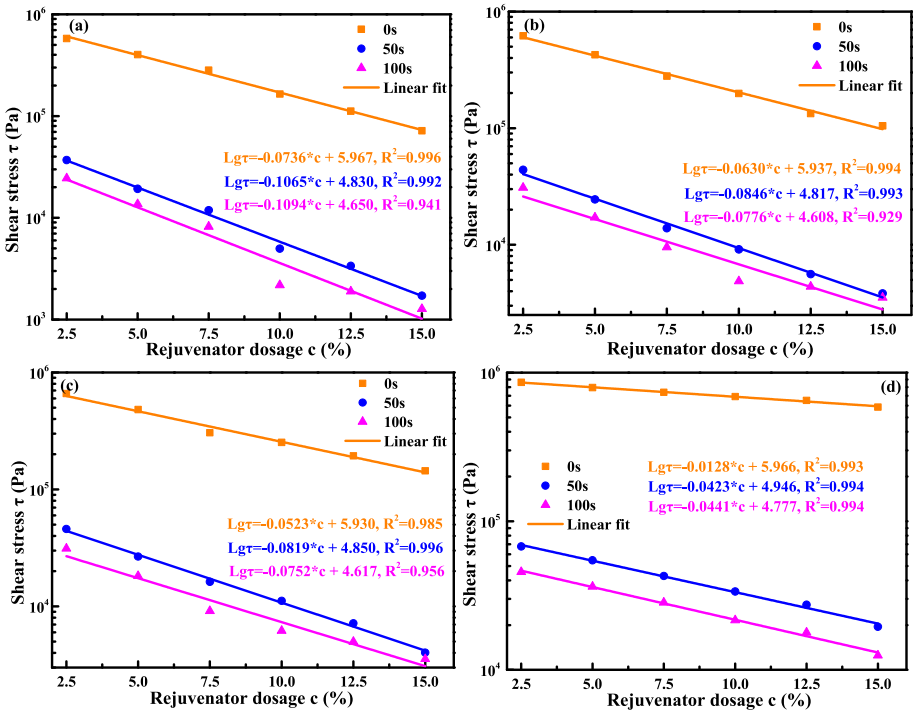

Fig. 5. Shear stress values of LAB40 rejuvenated bitumen (a) BORB; (b) EORB; (c) NORB; (d) AORB.

restoration level of aromatic-oil is much lower than the others. As the relaxation time prolongs from 0s to 50s, the τ value of rejuvenated bitumen decreases, but its sensitivity to rejuvenator dosage enlarges significantly. However, the increment in relaxation time from 50s to 100s has limited influence on the τ and Log(τ)-C correlation curves. Therefore, it is not necessary to consider both τ parameters at 50s and 100s for evaluating the rejuvenator type/dosage on the relaxation performance of rejuvenated bitumen.

The Log(τ)-C correlation curves of LAB20 and LAB80 rejuvenated bitumen can be found in Figs. S1 and S2. The corresponding correlation equations are summarized in Table 4. The absolute slope and intercept values decrease as the aging level deepens, indicating that rejuvenators show a lower rejuvenation efficiency on the relaxation performance restoration of aged bitumen with a more severe aging degree. Moreover, a high aging level remarkably enlarges the τ values of rejuvenated bitumen. It is observed that the sensitivity level of Log(τ) to rejuvenator dosage of rejuvenated bitumen with all aged binders increases as the relaxation time extends from 0s to 50s, but the difference is not significant between τ_{50s} and τ_{100s}. Furthermore, the influence level of relaxation time on the Log(τ)-C variation trend is the maximum, followed by the rejuvenator type and aging degree of bitumen.

Table 4
The correlation equations of Logτ-C curves of various rejuvenated binders.

Samples	Time	LAB20	LAB40	LAB80
BORB	0s	Logτ = -0.0732*C+5.852	−0.0736*C+5.967	−0.0574*C+5.960
	50s	Logτ = -0.1284*C+4.582	−0.1065*C+4.830	−0.0816*C+5.009
	100s	Logτ = -0.1589*C+4.468	−0.1094*C+4.650	−0.0921*C+4.926
EORB	0s	Logτ = -0.0749*C+5.860	−0.0630*C+5.937	−0.0505*C+5.934
	50s	Logτ = -0.1193*C+4.629	−0.0846*C+4.817	−0.0651*C+5.017
	100s	Logτ = -0.1132*C+4.411	−0.0776*C+4.608	−0.0663*C+4.878
NORB	0s	Logτ = -0.0523*C+5.869	−0.0523*C+5.930	−0.0408*C+5.959
	50s	Logτ = -0.0770*C+4.600	−0.0819*C+4.850	−0.0562*C+5.065
	100s	Logτ = -0.0788*C+4.414	−0.0752*C+4.617	−0.0555*C+4.919
AORB	0s	Logτ = -0.0141*C+5.866	−0.0128*C+5.966	−0.0093*C+5.961
	50s	Logτ = -0.0430*C+4.633	−0.0423*C+4.946	−0.0305*C+5.064
	100s	Logτ = -0.0444*C+4.448	−0.0441*C+4.777	−0.0321*C+4.928

3.2.2. Relaxation time t

Apart from the τ parameter, the relaxation time t is an important evaluation index for the relaxation performance of bituminous materials. Fig. 6 illustrates the relaxation time t with residue shear stress ratio of 75%, 50%, and 25% as a function of rejuvenator content. As the rejuvenator dosage increasing, all t values decline linearly. The rejuvenator type and residue stress ratio remarkably affect the Log(t)-C curves of rejuvenated bitumen. With the decrease of reside stress ratio, the t value and its sensitivity level to the rejuvenator dosage both enlarge. In addition, the bio-oil and aromatic-oil rejuvenated bitumen show the lowest and highest relaxation time, indicating the greatest and worst rejuvenation efficiency on relaxation time restoration of aged bitumen. Moreover, the engine-oil and naphthenic-oil rejuvenated binders exhibit similar t values. The sensitivity level of log(t) values to rejuvenator dosage for four rejuvenators follows bio-oil > aromatic-oil > naphthenic-oil > engine-oil, regardless of the residue shear stress ratio.

Apart from the rejuvenator type and dosage, the aging degree of bitumen would affect the interaction and rejuvenation level between the rejuvenators and aged bitumen. The Log(t)-C curves of LAB20 and LAB80 rejuvenated binders are presented in Figs. S3 and S4, and the relevant correlation formulas are listed in Table 5. As the aging level deepens, the intercept values in all correlation equations increase gradually, implying the high aging degree results in a long relaxation time of bitumen. It is interesting to note that the aging effect on the slope values depends on the rejuvenator type. With the aging level changes from LAB20 to LAB40 and LAB80, the absolute slope values of bio-oil and naphthenic-oil rejuvenated bitumen decrease and then increase,

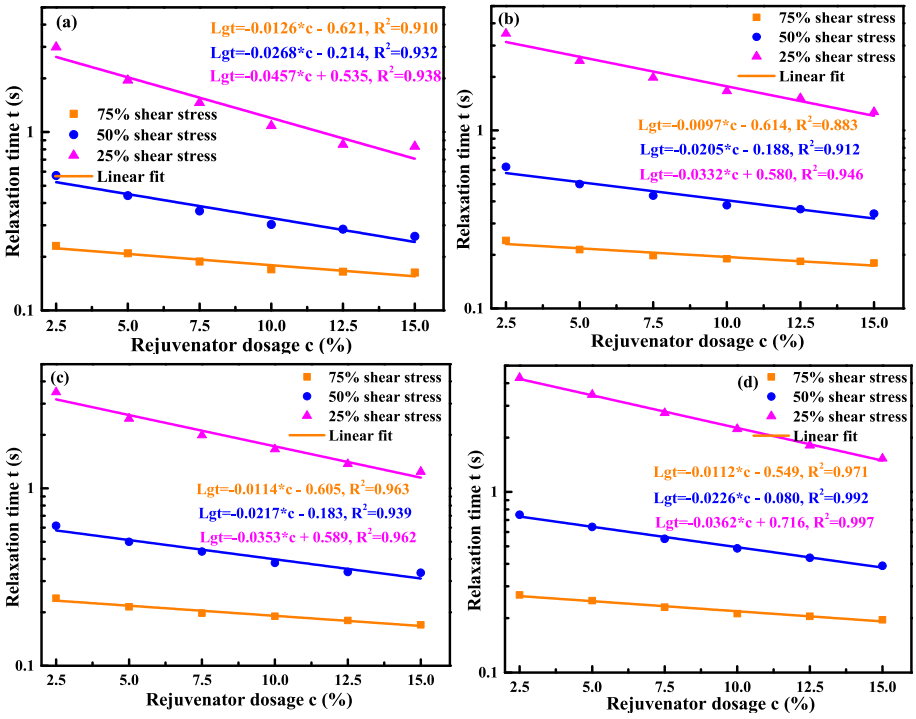

Fig. 6. Relaxation time values of LAB40 rejuvenated bitumen (a) BORB; (b) EORB; (c) NORB; (d) AORB.

Table 5
The correlation equations of Log(t)-C curves of various rejuvenated binders.

Samples	%	LAB20	LAB40	LAB80
BORB	75	Logt = -0.0168*C-0.652	−0.0126*C-0.621	−0.0145*C-0.535
	50	Logt = -0.0348*C-0.294	−0.0268*C-0.214	−0.0288*C-0.028
	25	Logt = -0.0572*C+0.378	−0.0457*C+0.535	−0.0459*C+0.851
EORB	75	Logt = -0.0124*C-0.656	−0.0097*C-0.614	−0.0089*C-0.521
	50	Logt = -0.0246*C-0.292	−0.0205*C-0.188	−0.0182*C+0.022
	25	Logt = -0.0426*C+0.391	−0.0332*C+0.580	−0.0256*C+0.915
NORB	75	Logt = -0.0126*C-0.645	−0.0114*C-0.605	−0.0132*C-0.481
	50	Logt = -0.0251*C-0.269	−0.0217*C-0.183	−0.0226*C+0.044
	25	Logt = -0.0391*C+0.418	−0.0333*C+0.589	−0.0353*C+0.971
AORB	75	Logt = -0.0080*C-0.635	−0.0112*C-0.549	−0.0091*C-0.507
	50	Logt = -0.0189*C-0.239	−0.0226*C-0.080	−0.0212*C+0.045
	25	Logt = -0.0313*C+0.459	−0.0362*C+0.716	−0.0331*C+0.924

while the AORB presents a converse trend. Meanwhile, the sensitivity level of Log(t) value to rejuvenator dosage of EORB tends to decrease as the aging level increases.

3.2.3. Shear stress ratio R

Fig. 7 displays the shear stress ratio R_{50s} and R_{100s} variations of LAB40 rejuvenated bitumen versus rejuvenator dosage. The R values tend to decline exponentially as the rejuvenator content rises. It means that the rejuvenated bitumen with a higher rejuvenator dosage would relax more thoroughly. Moreover, various rejuvenators show dissimilar restoration effects on the R parameter of aged bitumen. The BORB binder has the lowest R value, followed by NORB and EORB, while the AORB shows the highest value. It means the order of rejuvenation efficiency on the R parameter for four rejuvenators is BO > NO > EO > AO. Additionally, the increment in relaxation time reduces the R value and its dependence level on the rejuvenator dosage of rejuvenate binders. Figs. S5 and S6 demonstrate R–C curves of LAB20 and LAB80 rejuvenated binders, and the corresponding correlative equations are compared in Table 6. As the aging level prolongs, the R values of rejuvenated bitumen enlarge significantly for the increased stiffness and intermolecular interactions (Pei et al., 2023; Sun et al., 2018). Nevertheless, there is no clear relationship between the aging level and the variation rate of R–C curves of rejuvenated binders.

3.3. Influence of rejuvenator dosage and aging level on rejuvenation efficiency

This study calculates the rejuvenation percentage parameter (PR) using the relaxation indices of the virgin, aged, and rejuvenated binders.

$$PR = \frac{P_{aged} - P_{rejuvenated}}{P_{aged} - P_{virgin}} * 100 \quad (1)$$

where PR is the rejuvenation percentage, and P herein can be τ (shear stress-based), t (relaxation time-based), and R (stress ratio-based). Meanwhile, the P_{virgin}, P_{aged}, and $P_{rejuvenated}$ are the relaxation indices of virgin, aged, and rejuvenated binders, respectively.

3.3.1. Shear stress rejuvenation percentage τR

The effect of rejuvenator dosage on the τR of LAB40 rejuvenated binders is displayed in Fig. 8. It is observed that τR_{50s} and τR_{100s} of rejuvenated bitumen are extremely similar, and thus it is not necessary to measure both during the rejuvenation efficiency evaluation. Moreover, the τR_{0s} values are greatly larger than τR_{50s} and τR_{100s} parameters. For BORB, EORB, and NORB binder, the τR_{0s} scope is 0–400%, which is 140% for aromatic-oil rejuvenated bitumen with 15% AO dosage. Meanwhile, all τR_{50s} and τR_{100s} values of rejuvenated binders are lower than 150%. The magnitude of τR parameters of rejuvenated bitumen is BORB > EORB > NORB > AORB. It suggests that bio-oil rejuvenator shows the largest rejuvenation efficiency on the τR value of aged

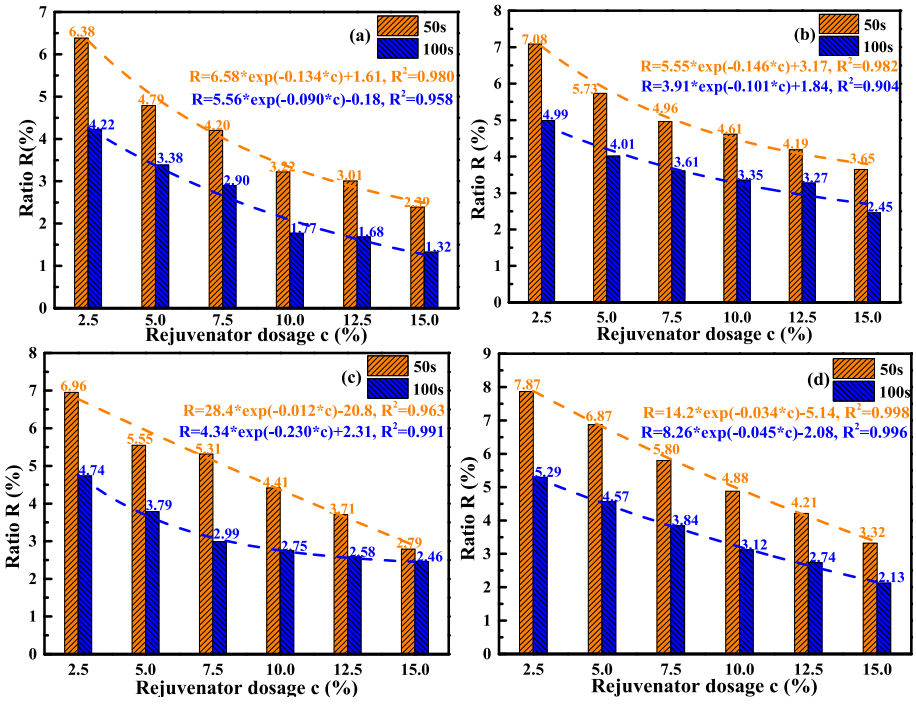

Fig. 7. Shear stress ratio values of LAB40 rejuvenated bitumen(a) BORB; (b) EORB; (c) NORB; (d) AORB.

Table 6
The correlation equations of R–C curves of various rejuvenated binders.

Samples		R_{50s} (%)	R_{100s} (%)
BORB	LAB20	R = 4.82*exp(-0.254*C) +1.24	R = 4.56*exp(-0.217*C)-0.14
	LAB40	R = 6.58*exp(-0.134*C) +1.61	R = 5.56*exp(-0.090*C) −0.18
	LAB80	R = 9.74*exp(-0.131*C) +3.55	R = 8.80*exp(-0.098*C) +0.81
EORB	LAB20	R = 6.45*exp(-0.076*C) −0.84	R = 2.42*exp(-0.163*C) +1.18
	LAB40	R = 5.55*exp(-0.146*C) +3.17	R = 3.91*exp(-0.101*C) +1.84
	LAB80	R = 7.83*exp(-0.087*C) +5.40	R = 7.09*exp(-0.059*C) +2.31
NORB	LAB20	R = 3.48*exp(-0.213*C) +2.70	R = 2.61*exp(-0.155*C) +1.32
	LAB40	R = 28.4*exp(-0.012*C) −20.8	R = 4.34*exp(-0.230*C) +2.31
	LAB80	R = 7.90*exp(-0.119*C) +6.32	R = 6.74*exp(-0.075*C) +3.17
AORB	LAB20	R = 9.27*exp(-0.038*C) −3.43	R = 2.78*exp(-0.177*C) +1.46
	LAB40	R = 14.2*exp(-0.034*C) −5.14	R = 8.26*exp(-0.045*C) −2.08
	LAB80	R = 10.97*exp(-0.082*C) +2.80	R = 7.89*exp(-0.099*C) +2.42

bitumen, while the aromatic-oil exhibits the weakest effectiveness. Interestingly, all τR parameters of BORB, EORB, and NORB binders increase exponentially as the rejuvenator dosage rises, while the AORB shows a linear relationship. Therefore, rejuvenator type affects the restoration level and the variation trend of τ parameter of rejuvenated bitumen to rejuvenator content.

The τR-C results of LAB20 and LAB40 rejuvenated bitumen can be found in Figs. S7 and S8. The aging degree of bitumen significantly influences the τR value and its sensitivity to rejuvenator dosage, but the ranking of rejuvenation efficiency on τ value for four rejuvenators keeps constant. Meanwhile, variation trends (exponentially or linearly) of τR values of rejuvenated bitumen to rejuvenator dosage are independent on the aging level of bitumen. The difference in τR_{50s} and τR_{100s} values of LAB20 rejuvenated bitumen is apparent, which cannot be detected in LAB40 and LAB80 cases. The increased aging degree reduces τR values of rejuvenated binders but enlarges its sensitivity level to rejuvenator dosage based on the parameters of correlation equations shown in Table 7. Although these three τ parameters can reflect the rejuvenation effects of various rejuvenators, the scope of τR_{0s} (0–700%) and τR_{100s} (−150-150%) deviates from the complex modulus G*-based rejuvenation percentages (0–150%). Therefore, the τ_{50s} is preferred as the most effective parameter for rejuvenation efficiency evaluation on the shear stress of rejuvenated bitumen during the relaxation process.

3.3.2. *Relaxation time rejuvenation percentage tR*

The rejuvenation percentages based on relaxation times tR of rejuvenated bitumen are displayed in Fig. 9. The increased rejuvenator dosage promotes the enlargement of tR values, and exponential relationships are observed. The BORB and AORB exhibit the largest and smallest tR parameters, respectively. It means that bio-oil shows the greatest potential to restore the relaxation performance of aged bitumen, while the aromatic-oil has the lowest effect, which agrees well with the τR results. Moreover, the tR values of EORB and NORB binders are similar and in between BORB and AORB. The tR values of all rejuvenated bitumen tend to decrease as the residue stress ratio reduces, especially at high rejuvenator dosages. However, the difference in $tR_{75\%}$, $tR_{50\%}$, and $tR_{25\%}$ of AORB binders is insignificant. Further, the rejuvenator type and residue stress ratio affect the sensitivity level of tR parameter to rejuvenator dosage according to exponential parameters in correlation equations. For BORB and AORB binder, the influence degree of rejuvenator dosage on tR values shows a decreasing trend with a reduction of residue stress ratio, which increases and then declines for EORB and NORB. Additionally, this phenomenon is more obvious for BORB. Interestingly, AORB binder exhibits the lowest tR but the highest dependence on rejuvenator dosage. Meanwhile, the residue stress ratio affects the sensitivity level of tR to rejuvenator content for BORB, EORB, and NORB.

The tR-C curves of LAB20 and LAB80 rejuvenated binders are drawn in Figs. S9 and S10, and all correlation equations are summarized in Table 8. Regardless of the aging degree of bitumen, the order of tR

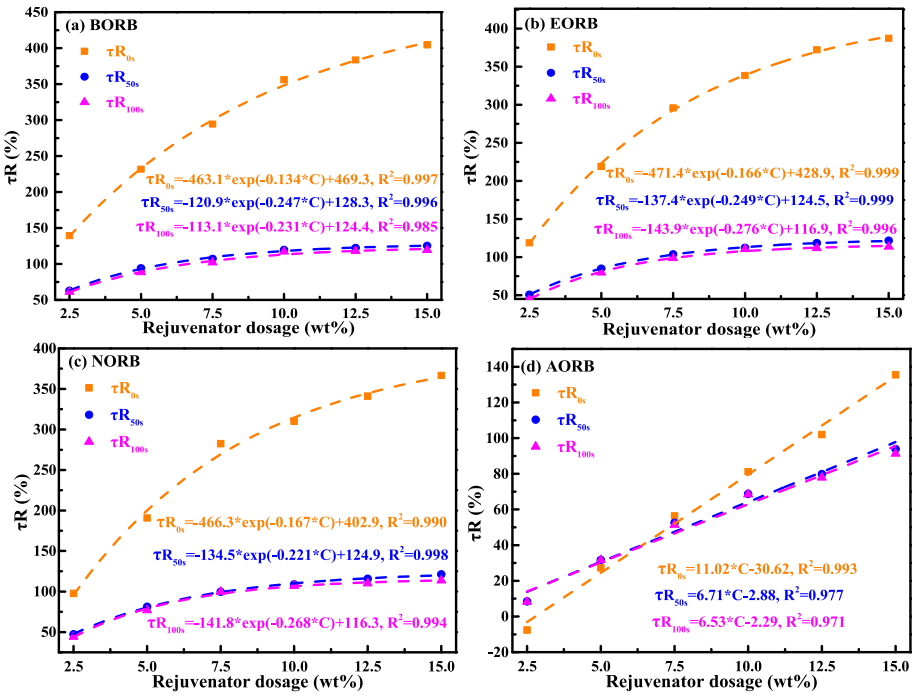

Fig. 8. The τR values of LAB40 rejuvenated bitumen.

Table 7
The correlation equations of τR-C curves of various rejuvenated binders.

Samples		τR_{0s} (%)	τR_{50s} (%)	τR_{100s} (%)
BORB	LAB20	−733*exp (-0.200*C) +738	−155*exp (-0.371*C) +153	−503*exp (-0.409*C) +238
	LAB40	−463*exp (-0.134*C) +469	−121*exp (-0.247*C) +128	−113*exp (-0.231*C) +124
	LAB80	−277*exp (-0.127*C) +302	−86*exp (-0.218*C) +111	−84*exp (-0.204*C) +110
EORB	LAB20	−765*exp (-0.166*C) +793	−153*exp (-0.271*C) +158	−396*exp (-0.279*C) +231
	LAB40	−471*exp (-0.166*C) +429	−137*exp (-0.249*C) +125	−144*exp (-0.276*C) +117
	LAB80	−265*exp (-0.147*C) +280	−88*exp (-0.194*C) +108	−85*exp (-0.201*C) +105
NORB	LAB20	−716*exp (-0.161*C) +689	−159*exp (-0.286*C) +141	−445*exp (-0.328*C) +179
	LAB40	−466*exp (-0.167*C) +403	−135exp (-0.221*C) +125	−142*exp (-0.268*C) +116
	LAB80	−284*exp (-0.085*C) +310	−89*exp (-0.146*C) +109	−85*exp (-0.150*C) +106
AORB	LAB20	16.51*C+58.75	9.00*C+16.71	25.27*C-162.2
	LAB40	11.02*C-30.62	6.71*C-2.88	6.53*C-2.29
	LAB80	4.61*C+27.39	3.38*C+33.23	3.35*C+33.31

parameter for rejuvenated bitumen follows BORB > EORB ≈ NORB > AORB. Nevertheless, the aging level remarkably affects the tR value and its variation rate versus rejuvenator content. As the aging degree of bitumen deepens from LAB20 to LAB40 and LAB80, the rejuvenator efficiency of all rejuvenators on relaxation time is weakened, and the sensitivity of tR values to rejuvenator dosage is enhanced. It can be found that three parameters ($tR_{75\%}$, $tR_{50\%}$, $tR_{25\%}$) can somewhat mirror the rejuvenation efficiency of various rejuvenators on relaxation time of aged bitumen, and the difference is detected but limited, especially for AORB. Therefore, three relaxation time parameters effectively indicate rejuvenation efficiency evaluation on relaxation behaviors. However, the magnitude of rejuvenation efficiency is constant for all relaxation time parameters. Thus, selecting relaxation time parameter with one residue stress ratio is recommended to assess the rejuvenation efficiency. This study chooses the t25% index as the effective evaluation indicator because it covers the most relaxation behavior of rejuvenated bitumen. It should be emphasized that the relaxation time parameter needs to be consistent to determine the difference in rejuvenation efficiency on relaxation performance of various rejuvenator-aged bitumen blends without the influence of residue stress ratio.

3.3.3. *Stress ratio rejuvenation percentage RR*

Fig. 10 displays the increasing variations of RR values at relaxation time of 50s and 100s as a function of rejuvenator dosage. The RR parameter and its variation trend of rejuvenated bitumen depend on the rejuvenator type/dosage and relaxation time. The RR_{50s} values of rejuvenated bitumen enlarge linearly as the rejuvenator content rises. Moreover, the RR_{100s} parameter of BORB and AORB also show a linearly increasing trend, while EORB and NORB binders present exponential relationships. However, the difference in RR_{50s} and RR_{100w} indices of rejuvenated bitumen is not tremendous, particularly for BORB and EORB binders. Within the whole rejuvenator dosage scope, the BORB has the highest RR value, indicating that bio-oil rejuvenator can maximally restore the relaxation stress ratio of aged bitumen. Meanwhile, the RR_{50s} values of EORB and NORB are larger than AORB, and the former is slightly smaller. Nevertheless, the RR_{100s} of AORB with high rejuvenator content are higher than that of NORB and EORB binders. In other words, the magnitude of RR_{100s} for four rejuvenators depends on the rejuvenator dosage. Thus, it is not appropriate to use the R_{100s} parameter for estimating the rejuvenation efficiency of various rejuvenators on the relaxation performance of aged bitumen, and the R_{50s} index is more effective. Further, the magnitude of increasing rate of RR_{50s} is AORB > NORB > BORB > EORB. It also will change the RR_{50s} ranking of various rejuvenated bitumen when the rejuvenator dosage exceeds a certain value.

The aging effect on the RR values of rejuvenated bitumen is shown in Figs. S11 and S12. Irrespective of aging degree, the RR_{50s} of all rejuvenated binders increase linearly versus the rejuvenator content. However, the variation law (linearly or exponentially) of RR_{100s} depends on the aging level and rejuvenator type. When aged bitumen is LAB80, the RR_{50s} and RR_{100s} parameters show a linearly increasing trend to rejuvenator dosage, while the difference in RR_{50s} and RR_{100s} values is limited. It indicates that the influence of relaxation time on the RR

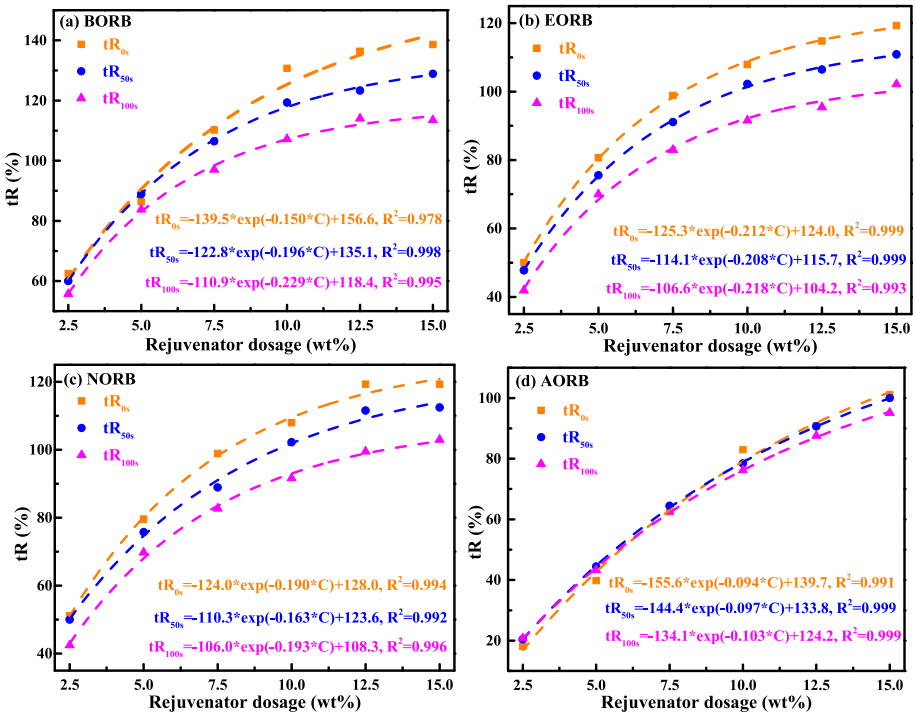

Fig. 9. The tR values of LAB40 rejuvenated bitumen.

Table 8
The correlation equations of tR-C curves of various rejuvenated binders.

Samples		$tR_{75\%}$ (%)	$tR_{50\%}$ (%)	$tR_{25\%}$ (%)
BORB	LAB20	−790*exp (-0.189*C) +504	−607*exp (-0.239*C) +392	−461*exp (-0.291*C) +250
	LAB40	−140*exp (-0.150*C) +157	−123*exp (-0.198*C) +135	−111*exp (-0.229*C) +118
	LAB80	−89*exp (-0.186*C) +112	−75*exp (-0.196*C) +105	−65*exp (-0.197*C) +101
EORB	LAB20	−549*exp (-0.261*C) +328	−492*exp (-0.267*C) +268	−412*exp (-0.289*C) +189
	LAB40	−125*exp (-0.212*C) +429	−114*exp (-0.208*C) +116	−107*exp (-0.218*C) +104
	LAB80	−65*exp (-0.182*C) +92	−60*exp (-0.174*C) +90	−55*exp (-0.176*C) +88
NORB	LAB20	−569*exp (-0.194*C) +354	−522*exp (-0.245*C) +262	−409*exp (-0.249*C) +176
	LAB40	−124*exp (-0.190*C) +128	−110*exp (-0.170*C) +124	−106*exp (-0.193*C) +108
	LAB80	−81*exp (-0.156*C) +98	−73*exp (-0.163*C) +93	−70*exp (-0.161*C) +92
AORB	LAB20	−529*exp (-0.099*C) +318	−509*exp (-0.115*C) +279	−429*exp (-0.123*C) +212
	LAB40	−156*exp (-0.094*C) +261	−144*exp (-0.097*C) +134	−134*exp (-0.130*C) +124
	LAB80	−219*exp (-0.014*C) +141	−88*exp (-0.056*C) +126	−66*exp (-0103*C) +98

parameter of aged bitumen disappears at a high aging level. Because of the consistency to variation law, the R_{50s} is more appropriate to effectively evaluate the rejuvenation efficiency of rejuvenated bitumen than the R_{100s} parameter. The correlation equations of RR-C curves are listed in Table 9. As the aging level increases, the RR_{50s} values and relative sensitivity to rejuvenator dosage of rejuvenated bitumen tend to decrease dramatically. The order of RR_{50s} of rejuvenated bitumen (BORB > NORB > EORB > AORB) keeps constant as variable aging level, affecting the magnitude of slope values. It may result in an order variation of RR_{50s} values of rejuvenated binders at a higher rejuvenator dosage.

3.4. Influence of aging and rejuvenation on the relaxation model of bitumen

The relaxation behavior resulting from the transformation and dissipation of internal energy can be described with the entropy equilibrium equation of Gibbs, shown as follows (Fu et al., 2016):

$$\rho T\frac{ds}{dt}=\rho T\frac{dQ}{dt}+\rho\frac{de}{dt}-\varepsilon\frac{d\sigma}{dt} \tag{2}$$

where, ρ and s are the density and entropy per unit mass of bituminous material; T and t refer to the temperature and relaxation time; Q and e represent the entropy increment and internal energy per unit mass; ε and σ show the shear strain and stress, respectively.

In this case, total entropy increment is caused by stress relaxation and reflected by the strain energy:

$$\rho T\frac{dS_i}{dt}=k\frac{dW}{dt} \tag{3}$$

where k denotes the conversion rate of irreversible entropy increment of strain energy, and W refers to the total strain energy.

At the same time, it was reported that the conversion rate of irreversible entropy increment of strain energy was associated with material and loading time (Xing et al., 2020).

$$k=mt^n \tag{4}$$

where m and n are the material parameters. Thus, Eq. (3) can be written as:

$$\rho T\frac{dS_i}{dt}=mt^n\frac{\varepsilon d\tau}{dt}=u \tag{5}$$

It should be mentioned that the shear strain is constant (1%), and $dW=\varepsilon d\tau$. After further integration, the correlation equation between ε and τ is expressed as:

$$\tau=\frac{ut^{1-n}}{\varepsilon m(1-n)}=\frac{At^{1-n}}{\varepsilon} \tag{6}$$

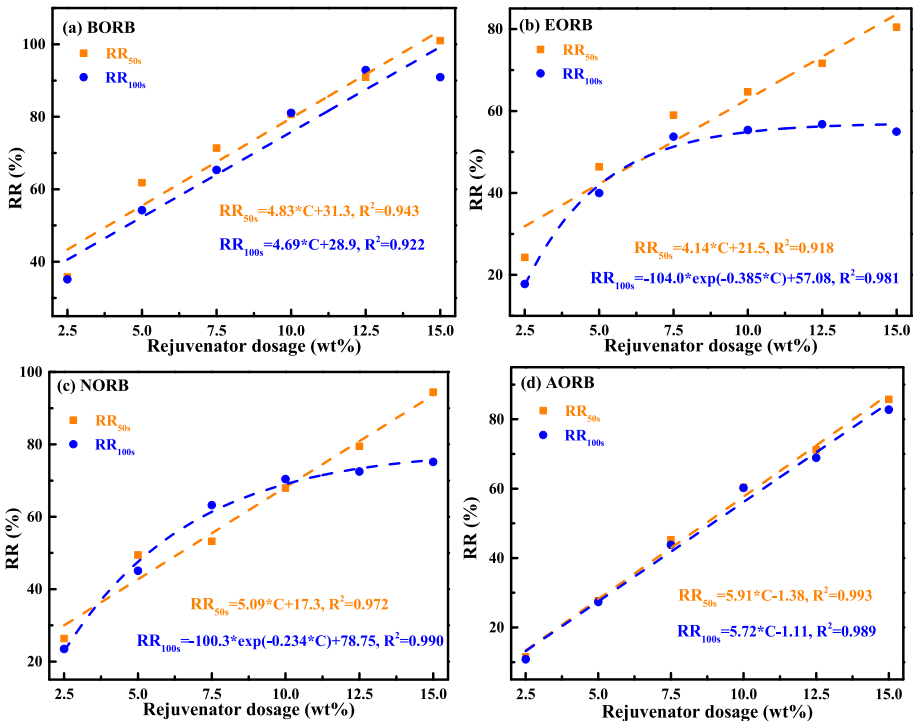

Fig. 10. The RR values of LAB40 rejuvenated bitumen.

Table 9
The correlation equations of RR-C curves of various rejuvenated binders.

Samples		RR_{50s} (%)	RR_{100s} (%)
BORB	LAB20	30.95*C-112.6	−514*exp(-0.234*C) +258
	LAB40	4.83*C+31.3	4.69*C+28.9
	LAB80	3.49*C+32.56	3.93*C+29.83
EORB	LAB20	30.26*C-155.6	−240*exp(-0.503*C) +14
	LAB40	4.14*C+21.5	−104*exp(-0.385*C) +57
	LAB80	2.62*C+23.50	2.78*C+22.65
NORB	LAB20	22.82*C-170.0	21.93*C-165.2
	LAB40	5.09*C+17.3	−100*exp(-0.234*C) +79
	LAB80	2.64*C+20.47	2.75*C+19.78
AORB	LAB20	24.9*C-185.4	−316*exp(-0.177*C) +90
	LAB40	5.91*C-1.38	5.72*C-1.11
	LAB80	3.57*C+21.15	3.53*C+21.18

where A is the material parameter, equal to u/m*(1-n).

The stress relaxation model based on thermodynamic theory was adopted to fit all relaxation curves of the virgin, aged, and rejuvenated bitumen. Moreover, the parameters A and n were used to quantitatively describe the aging and rejuvenation effects on the relaxation curve of aged bitumen.

Fig. 11 illustrates the τ-t curves and formulas of virgin and aged bitumen. High R^2 values (>0.99) indicate that proposed stress relaxation model can fit the relaxation curves of bituminous materials well. The parameters A and n show a distinct sensitivity to the long-term aging level of bitumen. As shown in Fig. 12, the parameters A and n relaxation model of bitumen increase and decrease linearly as the long-term aging time extends. In addition, the magnitude and sensitivity of parameter A to aging time are greater than parameter n. The correlation equations between aging time t with parameters A and n can be utilized to predict the relaxation curves of aged bitumen with other long-term aging degrees.

The relaxation curves and equations of LAB40 rejuvenated bitumen are illustrated in Fig. 13. It is noticed that relative information of LAB20 and LAB80 rejuvenated binders can be found in Supplementary Materials. According to relaxation model equations, relaxation behaviors of

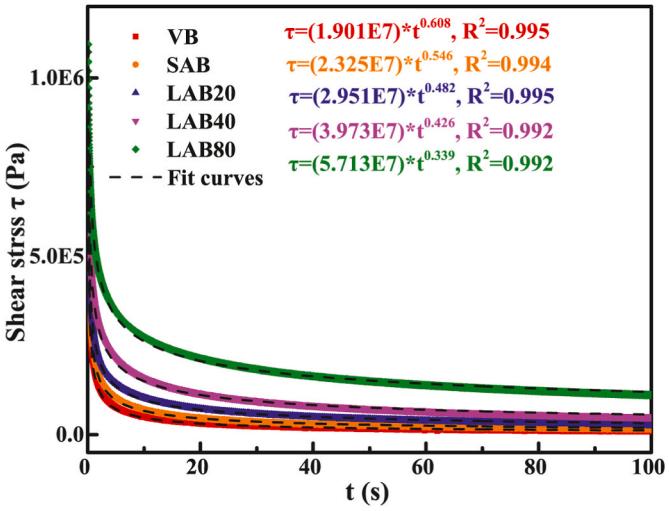

Fig. 11. The relaxation curves of virgin and aged bitumen.

rejuvenated bitumen are strongly influenced by rejuvenator type/dosage and aging degree of bitumen. The increment in rejuvenator dosage significantly reduces the shear stress and accelerates the relaxation rate of rejuvenated bitumen. Irrespective of aging level, bio-oil rejuvenator exhibits the greatest restoration level on relaxation performance of aged bitumen, followed by engine-oil and naphthenic-oil, while aromatic-oil shows the lowest efficiency.

The parameter A of rejuvenated bitumen and its corresponding rejuvenation percentage AR of rejuvenated bitumen are illustrated in Fig. 14. The A values of all rejuvenated binders tend to decline linearly as the rejuvenator dosage rises. Regardless of the aging degree, the magnitude of A parameter and sensitivity to rejuvenator dosage for rejuvenated bitumen follows BORB < EORB < NORB < AORB. As the aging degree increases, the A values of rejuvenated bitumen enlarge, but the effect of rejuvenator content reduces gradually. The AR values

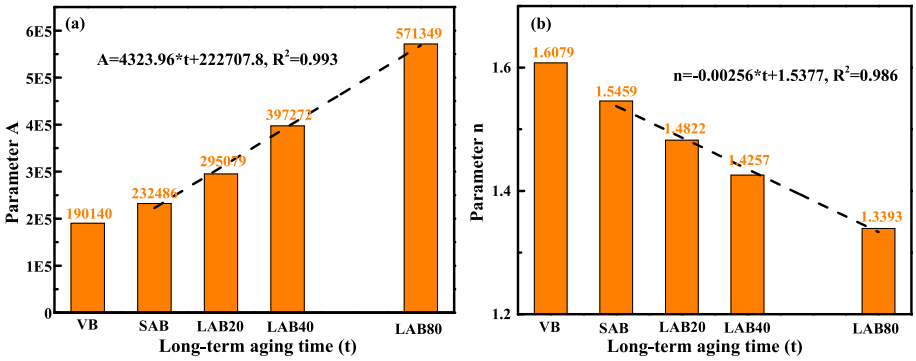

Fig. 12. Influence of long-term aging time on parameters A and n.

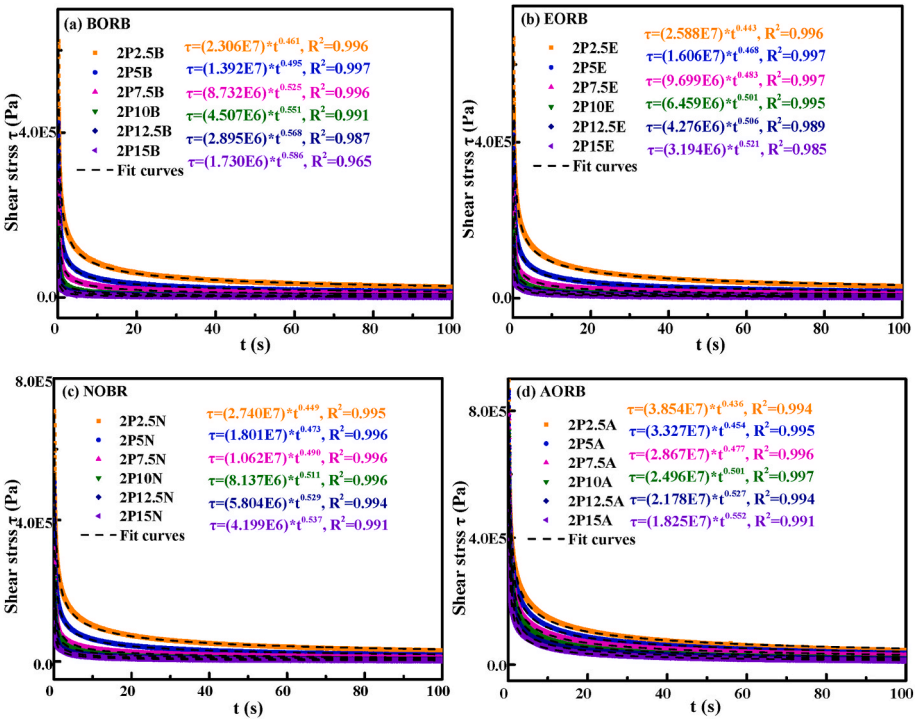

Fig. 13. The relaxation curves of LAB40 rejuvenated binders.

present exponentially increasing trends versus rejuvenator content. The BORB exhibits the largest AR values for all aged binders, followed by EORB and NORB, and AORB shows the lowest AR parameter. It implies that bio-oil rejuvenator can maximally restore the A value in the relaxation model equation of aged bitumen, while aromatic-oil displays the smallest rejuvenation efficiency on the A parameter. Additionally, the rejuvenation effectiveness of engine-oil and naphthenic-oil rejuvenators is in the middle, and the former has a greater value. As the aging level deepens, the AR values of rejuvenated binders remarkably decrease, indicating that rejuvenation efficiency of rejuvenators on A parameter is lower in an aged bitumen with a higher aging degree. It should be mentioned that rejuvenators can restore parameter A with increased sensitivity to rejuvenator type/dosage and aging level of bitumen. Therefore, the A parameter can be an effective index for evaluating the rejuvenation efficiency of various rejuvenator-aged bitumen blends.

Fig. 15 plots the correlation curves between rejuvenator dosage and parameter n in relaxation models of various rejuvenated binders. It is observed that the n values increase linearly as the rejuvenator dosage rises. The bio-oil rejuvenated bitumen has the largest n value. In contrast, the magnitude of the n parameter for engine-oil, naphthenic-oil, and aromatic-oil rejuvenated binders distinctly depends on the rejuvenator content and aging level of bitumen. The EORB bitumen shows a higher n value than NORB and AORB binder in LAB20, while AORB presents a larger n parameter than EORB, followed by NORB in LAB80. The aging degree negatively affects the n values of rejuvenated binders. It means that a high aging level would relieve the relaxation rate of bitumen. Meanwhile, the magnitude of rejuvenation efficiency of engine-oil, naphthenic-oil, and aromatic-oil rejuvenators on parameter n in the relaxation model of aged bitumen is sensitivity to the aging degree of bitumen dramatically. The nR results can reflect this finding. The bio-oil rejuvenator shows the largest rejuvenation efficiency in restoring the n parameter of aged bitumen. Overall, parameter n can effectively differentiate the rejuvenation efficiency of bio-oil from the others, but it fails to distinguish the engine-oil, naphthenic-oil, and aromatic-oil rejuvenators because of the high dependence of nR value to aging state of bitumen.

3.5. Further discussion on critical rheological parameters

A screening program (shown in Fig. 16) is developed to select the critical evaluation indicators, considering the rejuvenation possibility,

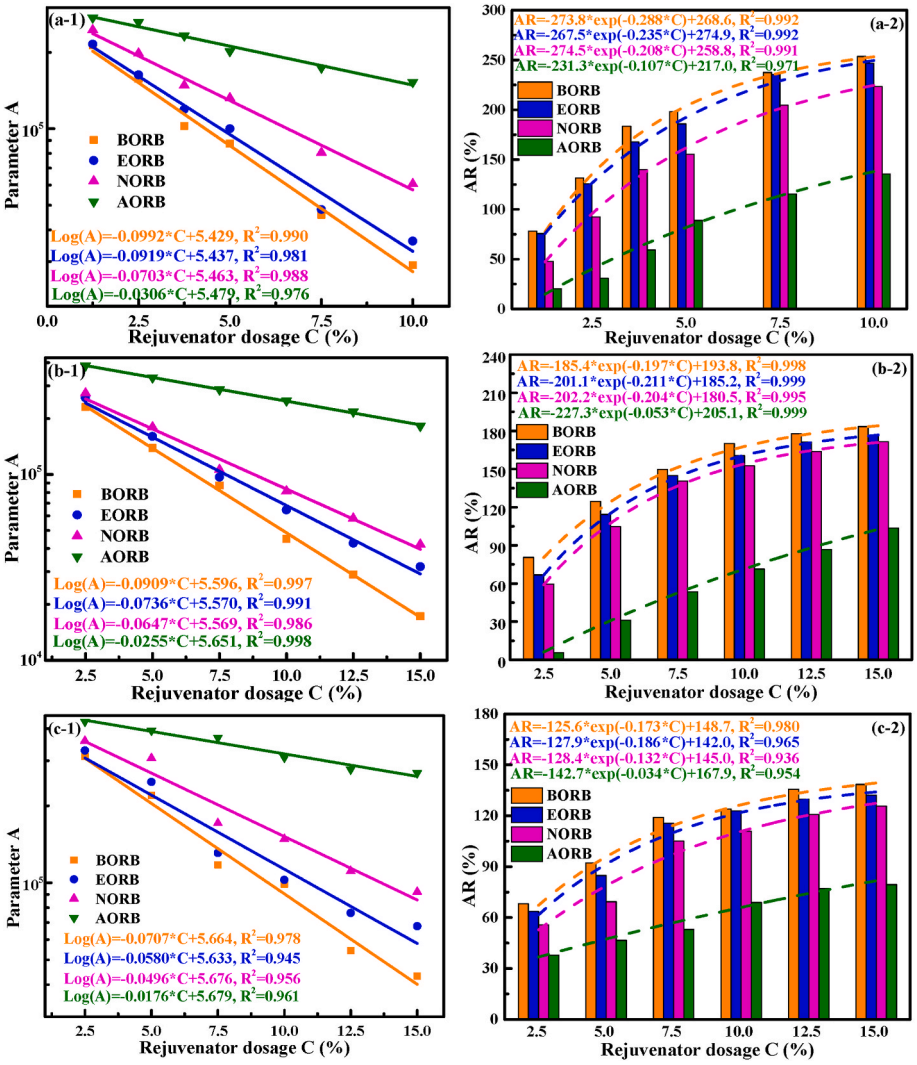

Fig. 14. The parameter A and AR values of various rejuvenated bitumen.

sensitivity degree to rejuvenator type/dosage and aging level, and the scope estimation of rejuvenation percentages. Table 10 lists the assessment results of different relaxation parameters in this study. The O and X represent the satisfied and unsatisfied results of these parameters to requirements. Additionally, one specific symbol ʘ is shown in the sensitivity of parameter A to rejuvenator dosage. The A-based rejuvenation percentages of rejuvenated binders have an exponentially increasing trend as rejuvenator content rises, which show a convergence at high rejuvenator dosage. Thus, the influence level of rejuvenator content on the A parameter restoration becomes insignificant as the rejuvenator dosage extends a certain value.

All relaxation parameters can be restored by adding rejuvenators. Interestingly, all shear stress τ and relaxation time t parameters meet the sensitivity requirements to rejuvenator type/dosage and aging level of bitumen, regardless of the relaxation time and residue stress state. However, their rejuvenation percentage regions are significantly different, which are 0–700%, 0–200%, -150-200%, 0–400%, 0–350%, and 0–200% to parameters τ_{0s}, τ_{50s}, τ_{100s}, $t_{75\%}$, $t_{50\%}$, and $t_{25\%}$. The high rejuvenation percentages of τ_{0s}, $t_{75\%}$, and $t_{50\%}$ are unexpected, and the minus value of τ_{100s} is nonpreferred. Moreover, the R_{50s} and R_{100s} parameters fail to be sensitive to rejuvenator type and aging level of bitumen. The relaxation model parameter A shows a great assessment result with a rejuvenation percentage scope of 0–250%, while the order of parameter n of rejuvenated bitumen strongly depends on the rejuvenator type and aging stage of bitumen. Therefore, the parameters τ_{50s}, $t_{25\%}$, and A are recommended as effective indicators for evaluating and comparing the rejuvenation efficiency of various rejuvenators on the relaxation performance recovery of aged bitumen.

3.6. Aging and rejuvenation effects on low-temperature sensitivity

Apart from material components, the relaxation performance of bituminous materials is also associated with temperature. This study performs the relaxation tests on three temperatures of 0, 10, and 20 °C to estimate the low-temperature susceptibility of various rejuvenated bitumen. The shear stress-based rejuvenation percentage τR values of LAB40 rejuvenated bitumen versus the reciprocal of temperature are shown in Fig. 17. The Log(τR) parameter exhibits a linear relationship with (1/T); however, the variation trend simultaneously depends on the rejuvenator type and dosage. For BORB, EORB, and NORB binders, their Log(τR) values enlarge linearly as the (1/T) rises, indicating the increased temperature weakens the rejuvenation efficiency of bio-oil, engine-oil, and naphthenic-oil rejuvenators on recovering the shear stress relaxation performance of aged bitumen, regardless of the rejuvenator dosage. The increase in rejuvenator dosage is expected to enhance the τR of rejuvenated bitumen, which is also influenced by the rejuvenator type. Meanwhile, the low-temperature sensitivity depends on the rejuvenator type and dosage. Based on the slope values, the low-temperature susceptibility of NORB is smaller than the EORB and BORB binders. In addition, the temperature sensitivity of these rejuvenated

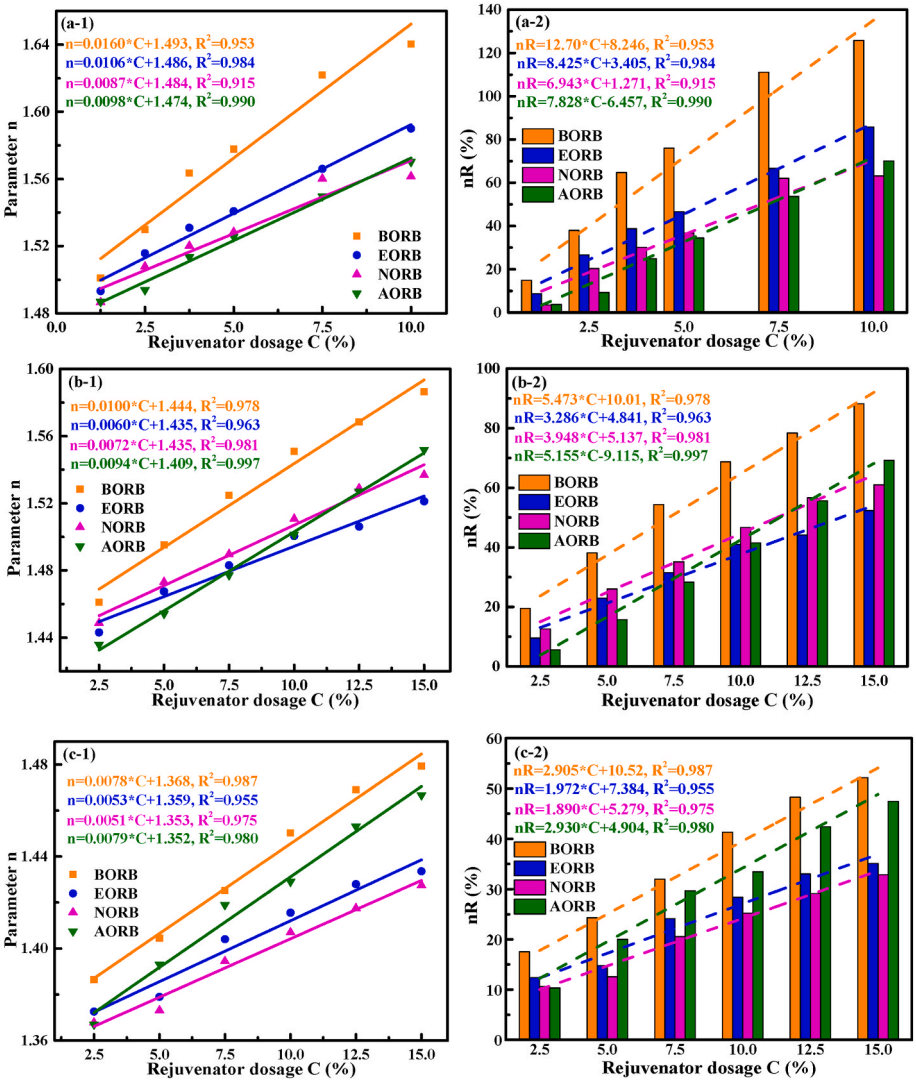

Fig. 15. The parameter n and nR values of various rejuvenated bitumen.

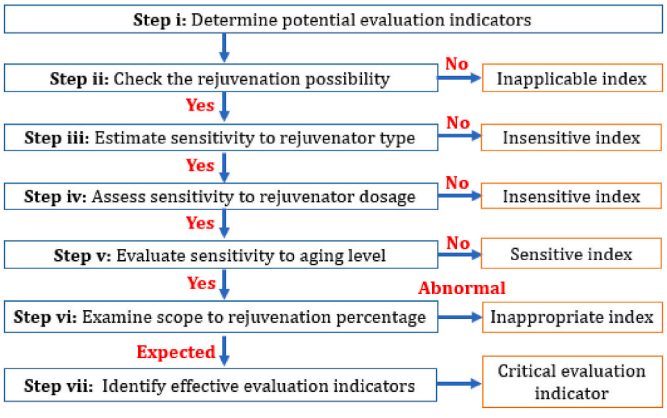

Fig. 16. Screening program for effective and critical evaluation indicators.

binders becomes more significant as the rejuvenator content increases. The Log(τR)-(1/T) curves of AORB binders differ from the others. When the aromatic-oil dosage is lower than 12.5%, the Log(τR) values reduce linearly as the (1/T) parameter increases, which shows the opposite trend when the aromatic-oil content is 12.5% and 15%. It implies that the rejuvenation efficiency of aromatic-oil on relaxation stress recovery of aged bitumen is greater at higher temperatures with low aromatic-oil content. The reason may be related to the deagglomeration effect of aromatic-oil on the asphaltene clusters in aged bitumen, which is limited for other rejuvenators.

The Ln(τR)-(1/T) curves of all rejuvenated bitumen are fitted with the Arrhenius equation:

$$\mathrm{Ln}(\tau R) = -\frac{E_a}{R}\frac{1}{T} + \mathrm{Ln}A \tag{7}$$

where Ea is the activation energy for relaxation behavior; and A shows the preexponential factor; R is the gas constant (8.314 J/mol·K^{-1}).

Table 11 summarizes the Ea, A, and R^2 values of all rejuvenated bitumen considering the influence of rejuvenator type/dosage and aging degree of bitumen. The magnitude of Ea values of rejuvenated bitumen is BORB < EORB < NORB < AORB. It manifests that it is the easiest for the BORB binder to do the relaxation work, while AORB shows the lowest relaxation possibility. The Ea values of aged bitumen decrease as the rejuvenator dosages rise but increase as the aging level deepens. Therefore, a high aging degree would hinder the relaxation behavior of bitumen by increasing the activation energy, which can be reduced by adding rejuvenators and restoring the relaxation capacity of aged bitumen molecules. Additionally, molecular structure (molecular weight, polarity, and mobility) of rejuvenators would be strongly related to their rejuvenation efficiency on relaxation performance of aged

Table 10
Analysis of critical rheological indicators for rejuvenation efficiency evaluation on low-temperature performance of rejuvenated bitumen.

Items	τ_{0s}	τ_{50s}	τ_{100s}	$t_{75\%}$	$t_{50\%}$	$t_{25\%}$	R_{50s}	R_{100s}	A	n
Recovery possibility	O	O	O	O	O	O	O	O	O	O
Sensitivity to rejuvenator type	O	O	O	O	O	O	X	X	O	X
Sensitivity to rejuvenator dosage	O	O	O	O	O	O	O	O	Θ	O
Sensitivity to aging level	O	O	O	O	O	O	X	X	O	X
Recovery percentage region (%)	0–700	0–200	−150–200	0–400	0–350	0–200	0–200	0–200	0–250	0–140

Note: O and X indicates Yes and No, respectively. In addition, Θ means Θ means Yes but the influence of rejuvenator dosage on AR values significantly reduces as the rejuvenator dosage rising.

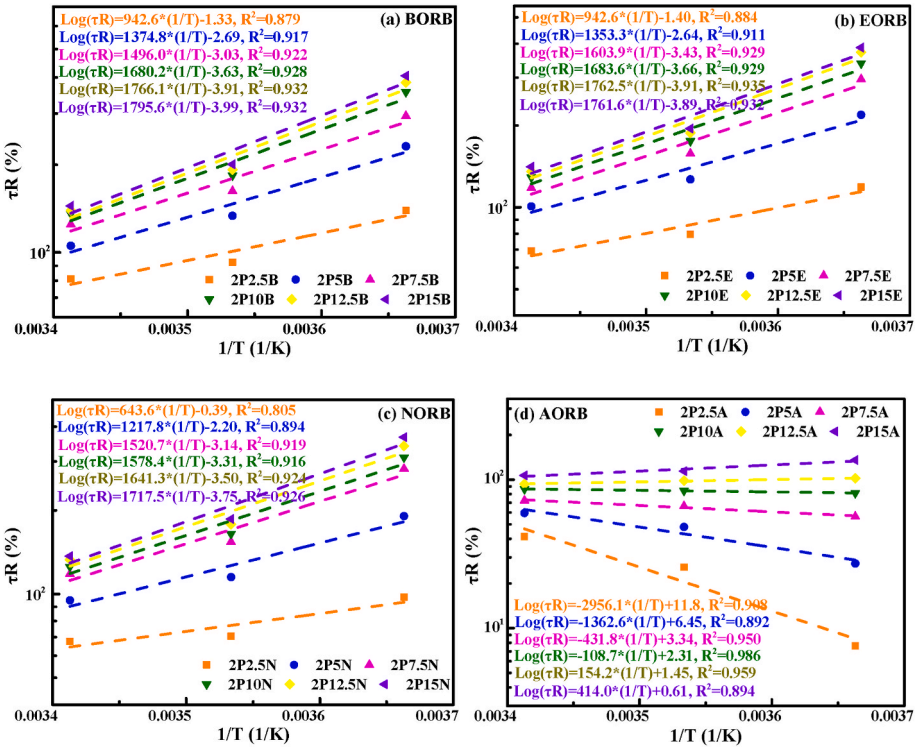

Fig. 17. Influence of temperature on τR values of rejuvenated binders.

bitumen, such as a huge difference in τR values and variation trends of AORB with the others (BORB, EORB, and AORB). It is vital to comprehensively analyze the molecular characteristics of these rejuvenators to fundamentally understand the mechanism for the difference in rejuvenation efficiency on relaxation behavior.

4. Molecular dynamic simulations outputs and discussion

The significant dependence of rejuvenation efficiency on the rejuvenator type has been detected based on relaxation tests. However, it is challenging to explore the underlying mechanism only from the difference in macroscale properties (such as density, viscosity, average molecular weight, or elemental compositions listed in Table 2). The relaxation performance of bituminous materials strongly relies on molecular mobility, intermolecular interaction, and free volume (Yao et al., 2022; Deng et al., 2022). Nevertheless, these molecular-scale thermodynamic properties of rejuvenators cannot be measured exactly in pavement engineering laboratories. Therefore, molecular dynamic (MD) simulation is adopted to predict these essential properties of rejuvenators and aged bitumen for answering the underlying reason why various rejuvenator-aged bitumen blends display different relaxation behaviors.

Molecular models of virgin bitumen, aged bitumen, and rejuvenators are shown in Fig. 18, determined based on a series of chemical characteristics (SARA fractions, element analysis, functional group distribution, molecular weight, etc.) The corresponding result can be found in our previous studies (Ren et al., 2021, 2022; M. Ren et al., 2022). It should be mentioned that experimental tests have validated the reliability of these established models. The COMPASSII force field is employed during the MD simulations to calculate the intermolecular interactions. Moreover, these bitumen and rejuvenator models are subjected to the isothermal-isobaric (NPT) and canonical ensemble (NVT) to achieve equilibrium at different temperatures. The time step and total simulation time for NPT and NVT processes are 1fs and 200ps, respectively. Moreover, the Nose thermostat and Andersen barostat are adopted to control the temperature and pressure of simulation systems. This study concentrates on the low-temperature relaxation-related properties (glass transition temperature Tg, molecular diffusion capacity, and free volume ratio) of aged bitumen and rejuvenator models.

4.1. Tg comparison of aged bitumen and rejuvenators

This study predicts the Tg values of various aged bitumen and rejuvenators based on the correlation between density values and simulation temperatures. Meanwhile, the DSC tests are performed on rejuvenators to measure and compare their Tg values with simulation results. Generally, glass transition temperature is defined as the temperature at which molecular mobility exhibits a phase transformation.

Table 11
The activation energy and pre-exponential factor of rejuvenated bitumen.

Samples	Ea (J/mol)	A	R^2	Samples	Ea (J/mol)	A	R^2
1P1.25B	−22765	7.079E-3	0.889	1P1.25E	−23989	4.074E-3	0.909
1P2.5B	−25109	4.266E-3	0.864	1P2.5E	−32439	1.698E-4	0.982
1P3.75B	−32714	2.188E-4	0.957	1P3.75E	−33116	1.738E-4	0.954
1P5B	−35500	6.918E-5	0.970	1P5E	−33457	1.660E-4	0.934
1P7.5B	−36897	4.786E-5	0.955	1P7.5E	−38549	6.918E-5	0.965
1P10B	−38300	2.884E-5	0.951	1P10E	−39989	1.349E-5	0.963
1P1.25N	−14471	1.738E-1	0.904	1P1.25A	17727	7.079E4	0.996
1P2.5N	−23476	6.026E-3	0.933	1P2.5A	19205	1.778E5	0.911
1P3.75N	−29975	5.623E-4	0.929	1P3.75A	4100	4.898E2	0.953
1P5N	−31612	3.020E-4	0.960	1P5A	−3457	8.710E-3	0.986
1P7.5N	−32892	2.344E-4	0.926	1P7.5A	−14999	2.512E-1	0.997
1P10N	−36246	6.026E-5	0.949	1P10A	−15026	2.692E-1	0.898
2P2.5B	−18045	4.677E-2	0.879	2P2.5E	−18045	3.981E-2	0.884
2P5B	−26318	2.042E-3	0.917	2P5E	−25907	2.291E-3	0.911
2P7.5B	−28639	9.333E-4	0.922	2P7.5E	−30704	3.715E-4	0.929
2P10B	−32165	2.344E-4	0.928	2P10E	−32230	2.188E-4	0.929
2P12.5B	−33809	1.230E-4	0.932	2P12.5E	−33740	1.230E-4	0.935
2P15B	−34374	1.023E-4	0.932	2P15E	−33723	1.288E-4	0.932
2P2.5N	−12321	4.074E-1	0.805	2P2.5A	56590	6.310E11	0.998
2P5N	−23313	6.310E-3	0.894	2P5A	26085	2.818E6	0.892
2P7.5N	−29111	7.244E-4	0.919	2P7.5A	8266	2.188E3	0.950
2P10N	−30216	4.898E-4	0.916	2P10A	2081	2.042E2	0.986
2P12.5N	−31420	3.162E-4	0.924	2P12.5A	−2952	28.18	0.959
2P15N	−32879	1.778E-4	0.926	2P15A	−7925	4.074	0.894
4P2.5B	−12679	3.715E-1	0.801	4P2.5E	−12091	4.571E-1	0.867
4P5B	−17570	6.166E-2	0.853	4P5E	−19090	3.020E-2	0.910
4P7.5B	−22252	1.072E-2	0.921	4P7.5E	−23344	6.918E-3	0.934
4P10B	−24021	5.370E-3	0.936	4P10E	−23518	6.310E-3	0.919
4P12.5B	−25377	3.311E-3	0.934	4P12.5E	−24980	3.802E-3	0.916
4P15B	−26542	2.089E-3	0.948	4P15E	−26253	2.291E-3	0.925
4P2.5N	−11982	5.495E-3	0.974	4P2.5A	8540	1.445E3	0.877
4P5N	−16585	9.120E-4	0.965	4P5A	9495	3.388E3	0.933
4P7.5N	−20042	4.074E-6	0.933	4P7.5A	−5519	4.898	0.833
4P10N	−22973	1.175E-6	0.926	4P10A	−1681	38.02	0.826
4P12.5N	−23524	7.943E-8	0.908	4P12.5A	−1158	1.380E2	0.92
4P15N	−24669	2.138E-8	0.901	4P15A	−4288	14.45	0.834

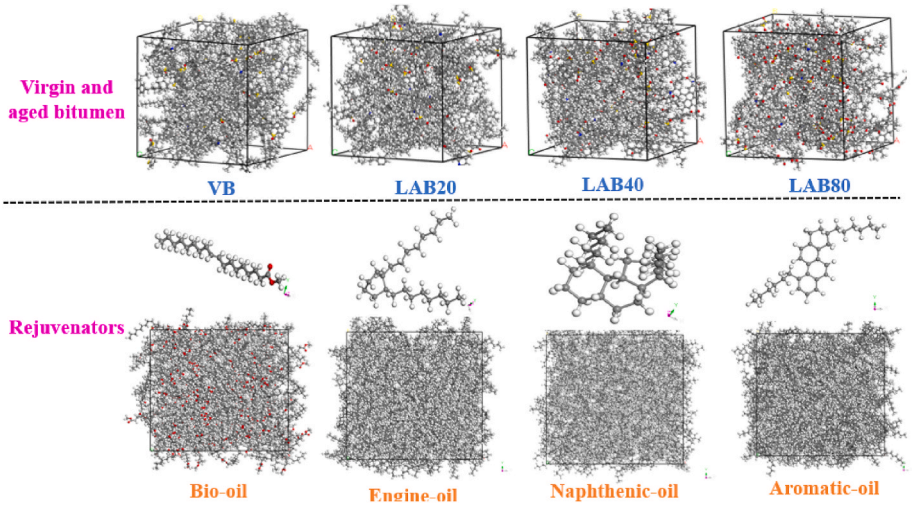

Fig. 18. Molecular models of aged bitumen and rejuvenators.

Before the Tg point (low temperature), the rigid molecules are hard to move due to insufficient energy. Afterward, the temperature dependence of physio-mechanical properties becomes more apparent. Herein, the density variation as a function of simulation temperatures for aged bitumen and rejuvenators is illustrated in Fig. 19. There are two different descending trends for density parameters as the temperature increases. The decreasing rate of density in the high-temperature region is much larger than that at low temperatures. The reason is that when the temperature exceeds the glass transition temperature point, the molecules are out from the boundary and move freely at high temperatures, leading to faster increment and reduced system volume and density, respectively. The magnitude of the density of virgin/aged bitumen is VB < LAB20 < LAB40 < LAB80 and the order for rejuvenators follows EO < BO < NO < AO. The density ranking results from the molecular weight and model volume relate to intermolecular interactions and molecular mobility.

The density parameter presents a segmented linear relationship with temperature in the whole temperature range, and the corresponding

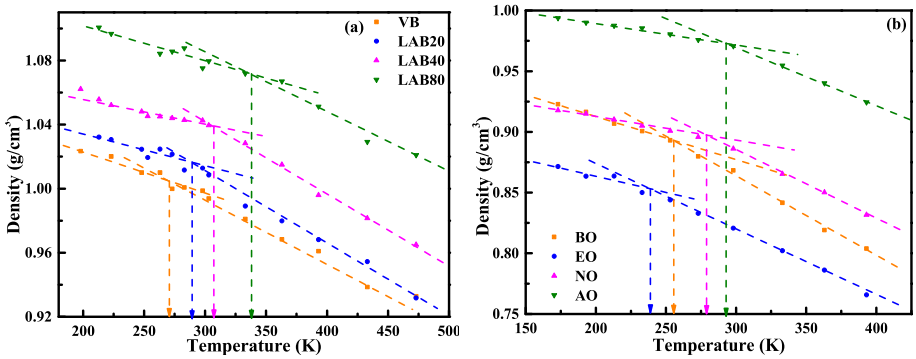

Fig. 19. The density-temperature curves of virgin/aged bitumen and rejuvenators.

equations are listed in Table 12. The R^2 higher than 0.90 refers to sufficient fitting accuracy. Besides, higher absolute value of equation slope represents the larger temperature sensitivity. The absolute slope values in equation (2) are higher than in equation (1) for all aged bitumen and rejuvenators. It implies that when the temperature exceeds the Tg point, the temperature sensitivities of aged bitumen and rejuvenators become more significant. There is no clear relationship between temperature sensitivity of density and aging degree of bitumen. Moreover, bio-oil rejuvenator is the most sensitive to temperature variation, followed by engine-oil and naphthenic-oil rejuvenator, while the density value of aromatic-oil exhibits the smallest temperature sensitivity. The turning point in equations (1) and (2) is glass transition temperature, and predicted Tg values of VB, LAB20, LAB40, and LAB80 are −3.43 °C, 4.03 °C, 34.98 °C, and 56.98 °C. The Tg values of bio-oil, engine-oil, naphthenic-oil, and aromatic-oil rejuvenator are predicted as −13.74 °C, −35.83 °C, 11.69 °C, and 20.82 °C, respectively.

Fig. 20 shows the DSC curves of virgin and aged bitumen to measure their experimental Tg values. The heat flow variation was detected, and the glass transition temperatures (Tg_{onset}, Tg, and Tg_{end}) are also presented. The heat flow increases gradually as the temperature rises. For all bitumen samples, the Tg parameter is determined by monitoring the turning point where the variation rate of heat flow versus temperature changes significantly. Only one Tg point with the Tg_{onset} and Tg_{end} values is observed for virgin and aged bitumen, also marked in DSC curves. As the aging degree deepens, the Tg value of bitumen enlarges dramatically. The reason is that oxidation aging increases the polarity, molecular weight, and intermolecular force of bitumen molecules. More energy is required to surmount the external and self-constraints for molecular motion.

The DSC curves of various rejuvenators are plotted in Fig. 21. The heat flow behaviors of engine-oil and naphthenic-oil rejuvenators are similar, showing only one turning point. However, bio-oil and aromatic-oil rejuvenators display different heating flow behaviors, and other obvious peaks are observed. For bio-oil rejuvenator, a wide (−31.25 °C–10.04 °C) and strong heat flow peak at −9.63 °C is detected, which may be related to the deagglomeration phenomenon of bio-oil molecules containing the polar ester functional group (S. Ren et al., 2022). On the other hand, three key points can be found in aromatic-oil rejuvenator: 26.55 °C, −19.21 °C, and 20.06 °C. The aromatic-oil comprises predominate aromatics, the more or less lightweight fraction (saturate), and heavy components (resins and asphaltenes). The turning points of −19.21 and 20.06 °C may be associated with the phase transition behaviors of resin and asphaltene molecules in the aromatic-oil rejuvenator.

Table 12
The correlation equations of density-temperature for various rejuvenators.

Samples	Equation (1)	R^2	Equation (2)	R^2
Virgin bitumen	ρ = -2.8304E-4*T + 1.0810	0.943	ρ = -3.7135E-4*T + 1.1048	0.988
LAB20	ρ = -2.5226E-4*T + 1.0867	0.918	ρ = -4.2327E-4*T + 1.1341	0.992
LAB40	ρ = -1.8697E-4*T + 1.0955	0.917	ρ = -4.4936E-4*T + 1.1763	0.993
LAB80	ρ = -2.2318E-4*T + 1.1464	0.934	ρ = -3.9965E-4*T + 1.2075	0.969
Bio-oil	ρ = -3.7612E-4*T + 0.9881	0.995	ρ = -6.6082E-4*T + 1.0619	0.992
Engine-oil	ρ = -3.5357E-4*T + 0.9323	0.996	ρ = -5.6754E-4*T + 0.9832	0.997
Naphthenic-oil	ρ = -2.2486E-4*T + 0.9576	0.993	ρ = -5.4747E-4*T + 1.0552	0.998
Aromatic-oil	ρ = -1.7314E-4*T + 1.0241	0.975	ρ = -4.8677E-4*T + 1.1163	0.999

Table 13 summarizes the measured and predicted Tg values of virgin/aged bitumen and various rejuvenators. It is denoted that there is a certain gap between MD simulation outputs and experimental results. The predicted Tg values of all virgin/aged bitumen and rejuvenators are higher than the DSC results. In detail, the outputted Tg results of VB, LAB20, LAB40, and LAB80 aged bitumen are 11.06 °C, 17.39 °C, 46.52 °C, and 65.52 °C larger than the measured values. Meanwhile, the Tg value from MD simulations for bio-oil, engine-oil, naphthenic-oil, and aromatic-oil rejuvenators are 31.95 °C, 16.64 °C, 51.39 °C, and 47.37 °C higher than experimental one, respectively. There are many reasons for the huge difference. Firstly, the average molecular models of bitumen and rejuvenators are established in this study, resulting in the negligence of lightweight molecules and an increase in Tg values. Secondly, the MD simulation outputs have fluctuations, and the scale gap would also contribute to the huge variation of the Tg parameter. Lastly, the Tg value from the DSC test with the limited lowest temperature of −70 °C may also be measured inaccurately. However, it is worth noting that the sequence of Tg values for virgin/aged bitumen and rejuvenators from MD simulations and experiments are the same. The aromatic-oil rejuvenator has the highest Tg value, followed by naphthenic-oil and bio-oil, while the engine-oil rejuvenator shows the lowest Tg value.

This finding agrees well with the experimental conclusion that the aromatic-oil rejuvenator exhibits the smallest rejuvenation efficiency on relaxation performance recovery of aged bitumen, followed by the naphthenic-oil, while the engine-oil and bio-oil show better rejuvenation effectiveness. In addition, the increased Tg of aged bitumen as the aging level deepens contributes to the reduced rejuvenation percentages of rejuvenators. It should be mentioned that the Tg value of engine-oil is slightly lower than the bio-oil rejuvenator, but the BORB binder shows a greater rejuvenation efficiency on relaxation properties than the EORB. It means that although the Tg parameter can explain the difference in rejuvenation effectiveness of various rejuvenators to some extent, the relaxation performance of rejuvenated binders is complicated and associated with molecular mobility, intermolecular interactions, and free volume fraction.

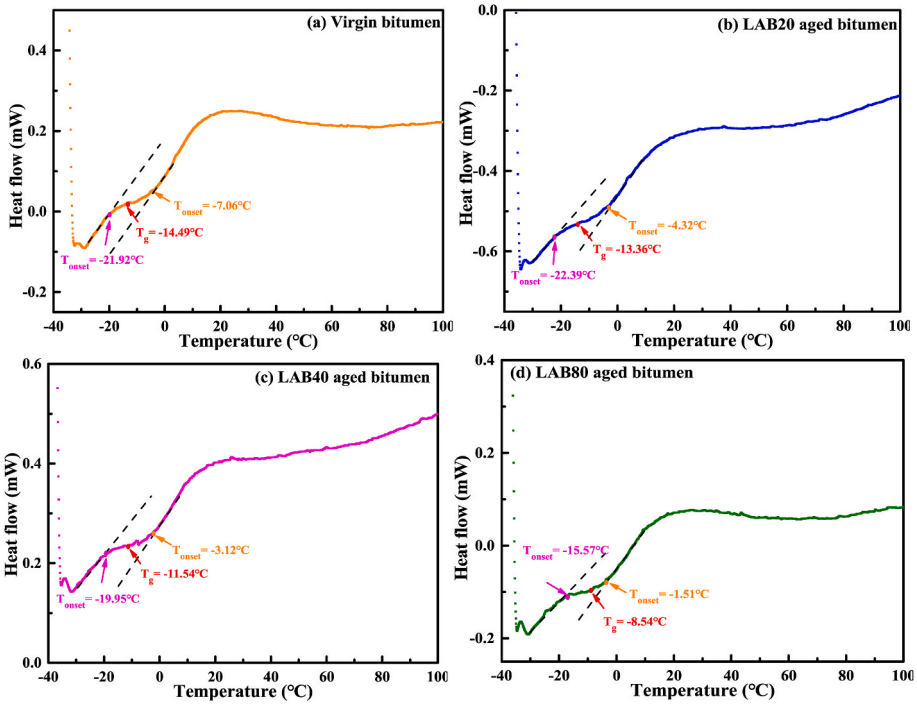

Fig. 20. The DSC curves of virgin and aged bitumen.

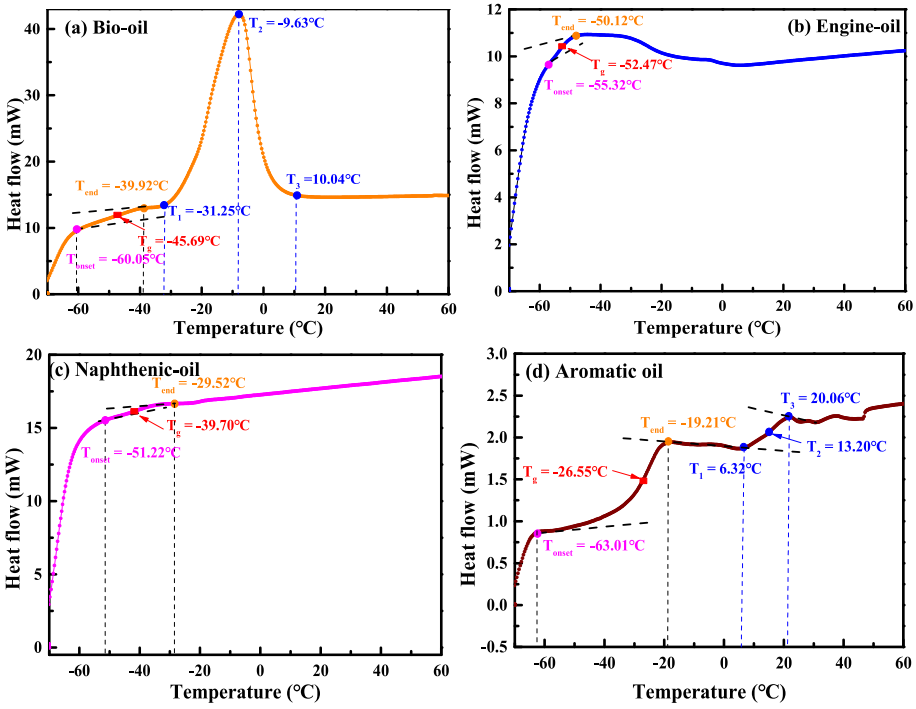

Fig. 21. The DSC curves of four rejuvenators.

4.2. Molecular self-diffusion capacity

The mean square displacement (MSD) of bitumen and rejuvenator molecules can be outputted from MD simulations, which refer to the molecular mobility and are described as:

$$MSD(t) = < \Delta r_i(t)^2 > = < [r_i(t) - r_i(0)]^2 > \quad (8)$$

where MSD(t) represents the mean square displacement of molecules at simulation time t (ps), Å^2; $r_i(t)$ and $r_i(0)$ show the current and initial coordinate, Å.

The dynamic behavior is strongly affected by the temperature, and high temperatures provide more kinetics energy and promote molecular mobility (Sun et al., 2018; Yao et al., 2022). The MSD-t curves of virgin/aged bitumen at different temperatures from 248K to 393K are displayed in Fig. 22. The linear correlation equations between MSD value and simulation time (>50ps) are also listed. As expected, the MSD values of all bitumen models enlarge as the simulation temperature

Table 13
Tg values of virgin/aged bitumen and rejuvenators.

Items	Bitumen	VB	LAB20	LAB40	LAB80
Experiment	Tg_{onset} (°C)	−21.92	−22.39	−19.95	−15.57
	Tg_{end} (°C)	−7.06	−4.32	−3.12	−1.51
	Tg (°C)	−14.49	−13.36	−11.54	−8.54
MD simulation	Tg (°C)	−3.43	4.03	34.98	56.98
	Rejuvenator	BO	EO	NO	AO
Experiment	Tg_{onset} (°C)	−60.05	−55.32	−51.22	−33.01
	Tg_{end} (°C)	−39.92	−50.12	−29.52	−19.21
	Tg (°C)	−45.69	−52.47	−39.70	−26.55
MD simulation	Tg (°C)	−13.74	−35.83	11.69	20.82

increases, particularly when the temperature exceeds 333K. It indicates that the movement of rejuvenator molecules intensifies at high temperatures. In addition, the MSD values of bitumen molecules present a distinct reduction trend as the aging level deepens, indicating that the aging degree negatively affects bitumen molecules' molecular mobility. Fig. 23 illustrates the MSD variations of various rejuvenators at different temperatures from 213K to 393K. At all temperatures and simulation time, the MSD values of the bio-oil rejuvenator are the largest, followed by engine-oil and naphthenic-oil, while the aromatic-oil shows the lowest MSD values. It indicates that the ranking of molecular mobility for four rejuvenators is BO > EO > NO > AO. The low molecular mobility of naphthenic-oil and aromatic-oil results in their unsatisfied rejuvenation efficiency on the low-temperature relaxation performance of aged bitumen. It is worth mentioning that the bio-oil rejuvenator shows greater molecular mobility than the engine-oil, although the latter has a lower Tg value. Therefore, the influence of molecular mobility is more dominant to the rejuvenation efficiency on relaxation behaviors of rejuvenated binders than the Tg parameter.

To further quantitatively estimate the molecular mobility of different rejuvenators, their diffusion coefficient values at different temperatures are calculated using Eq. (9), and the results are summarized in Table 14.

$$D = \frac{1}{6N}\lim_{t\to\infty}\frac{d}{dt}\sum MSD(t) = \frac{a}{6} \tag{9}$$

where D shows the diffusion coefficient, m^2/s; N refers to the total amount of bitumen or rejuvenator molecules; MSD and t are the mean square displacement ($Å^2$) and simulation time (s); and a is the slope parameter in MSD-t correlation equation.

The increased temperature markedly enlarges the diffusion coefficient of virgin/aged bitumen and rejuvenator molecules. High-temperature supplies more energy to rejuvenator molecules and increases their kinetic energy (Sun et al., 2018). For instance, when the temperature rises from 213K to 393K, the diffusion coefficient of bio-oil, engine-oil, naphthenic-oil, and aromatic-oil rejuvenator increases from 2.883E-11 m^2/s, 1.745E-11 m^2/s, 1.630E-11 m^2/s, and 1.165E-11 m^2/s to 9.303E-10 m^2/s, 5.590E-10 m^2/s, 3.978E-10 m^2/s, and 2.558E-10 m^2/s, respectively. The D values of bitumen reduce distinctly as the aging level increases, and all rejuvenators exhibit a higher diffusion coefficient than the virgin/aged bitumen. That's why adding all rejuvenators can restore the low-temperature relaxation property of aged bitumen. Meanwhile, at all simulation temperatures, the magnitude order of diffusion coefficient for four rejuvenators is as follows: BO > EO > NO > AO. This ranking is the same as the magnitude of rejuvenation efficiency for various rejuvenator-aged bitumen blends. Therefore, the D parameter of rejuvenators predicted from MD simulations can be used to preliminarily judge the ranking of rejuvenation efficiency of various rejuvenators on relaxation performance recovery of aged bitumen. It is essential to explore complex relationships between the experimental relaxation properties with thermodynamic parameters (such as Tg and D) outputted from MD simulations.

Generally, the Arrhenius equation is utilized to evaluate the relationship between diffusion coefficient and temperature, which is described as follows:

$$D = A\exp\left(\frac{-E_a}{RT}\right) \tag{10}$$

where D is the diffusion coefficient, m^2/s; Ea (J/mol) and T (K) refer to the activation energy and temperature; A is the pre-exponential factor, and R represents the universal gas constant (8.314 $J/mol{\cdot}K^{-1}$).

Fig. 24 illustrates the correlation curves and equations between temperature and diffusion coefficient of virgin/aged bitumen and rejuvenators according to Eq. (10). Meanwhile, the calculated Ea and A

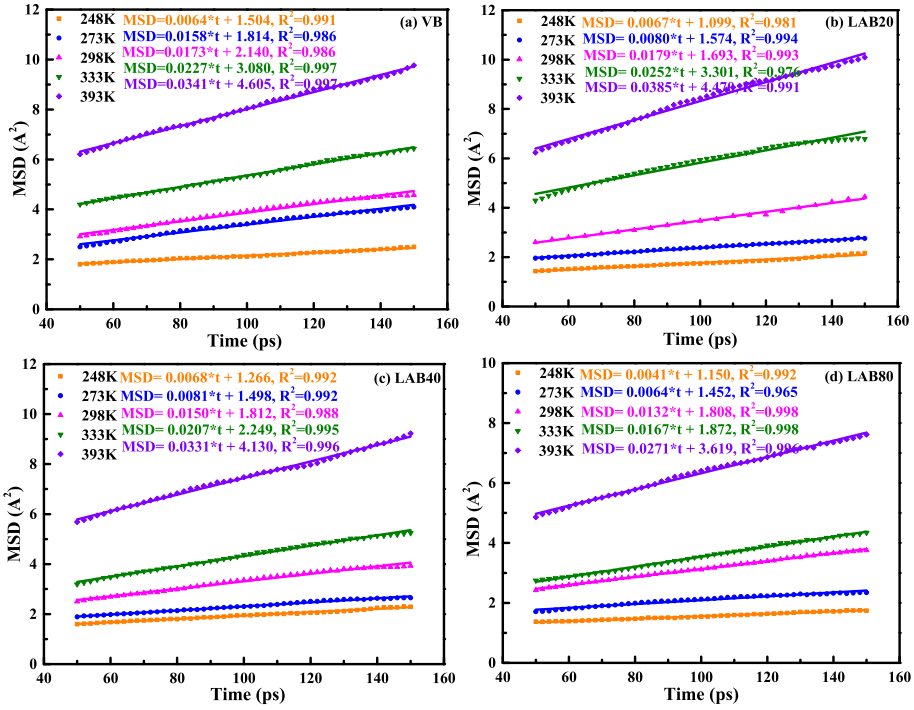

Fig. 22. The MSD curves of the virgin (a) and aged bitumen (b)–(d).

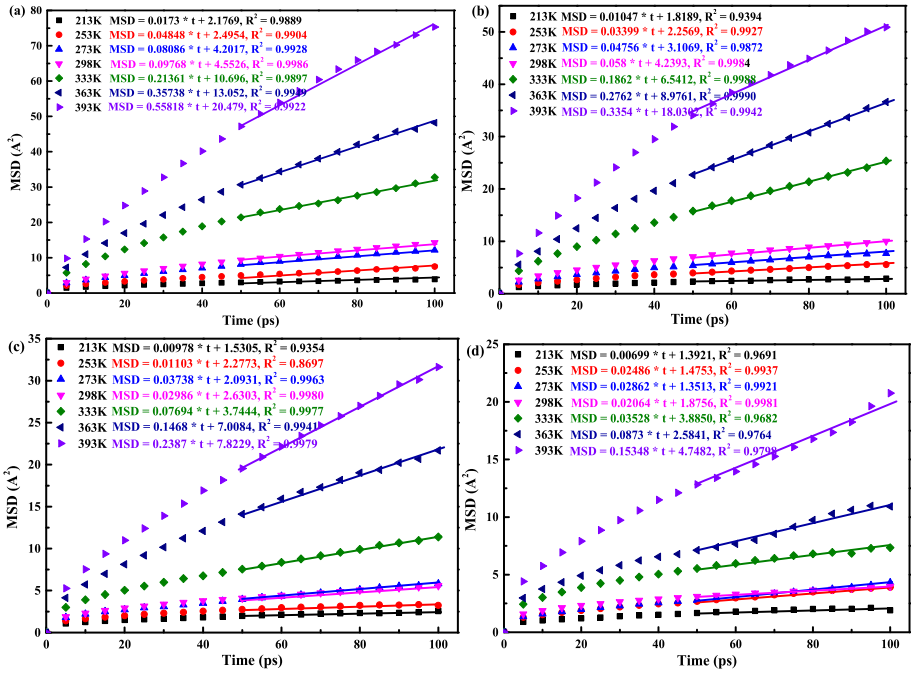

Fig. 23. The MSD curves of bio-oil (a), engine-oil (b), naphthenic-oil (c), and aromatic-oil (d) rejuvenators.

Table 14
The diffusion coefficient (m^2/s) of virgin/aged bitumen and rejuvenators.

Bitumen	VB	LAB20	LAB40	LAB80
253K	1.57E-11	1.31E-11	1.13E-11	6.75E-12
273K	2.13E-11	1.89E-11	1.72E-11	1.07E-11
298K	2.88E-11	2.55E-11	2.50E-11	1.92E-11
333K	3.79E-11	3.65E-11	3.45E-11	2.78E-11
393K	5.73E-11	5.78E-11	5.52E-11	4.51E-11
Rejuvenators	BO	EO	NO	AO
253K	8.080E-11	5.665E-11	3.838E-11	2.143E-11
273K	1.348E-10	7.927E-11	6.230E-11	4.770E-11
298K	1.628E-10	9.667E-11	8.977E-11	5.140E-11
333K	3.560E-10	3.103E-10	1.282E-10	5.880E-11
393K	9.303E-10	5.590E-10	3.978E-10	2.558E-10

values are listed in Table 15. The predicted Log(D) values of bitumen and rejuvenator models show a linear decreasing trend with the (1/T) extends, which is opposite to the Log(τR)-(1/T) curves of rejuvenated binders. Based on the absolute slope values, the order of temperature sensitivity for four rejuvenators is BO > EO > NO > AO, which is the same as the temperature susceptibility ranking of various rejuvenated binders from Log(τR)-(1/T) correlation formulas. Therefore, the Log(D)-(1/T) curves can be used to predict the temperature sensitivity of various

Table 15
The Ea and A values of virgin/aged bitumen and rejuvenators.

Bitumen	VB	LAB20	LAB40	LAB80
Ea (J/mol)	7237.34	8296.87	8829.88	10797.56
A	5.236E-6	7.283E-6	8.377E-6	1.314E-5
Rejuvenator	BO	EO	NO	AO
Ea (J/mol)	6198.16	6279.25	7922.05	8190.54
A	6.587E-8	4.737E-8	1.628E-7	5.727E-8

rejuvenator-aged bitumen systems.

The aging degree accelerates the increase in activation energy Ea values of bitumen. It indicates that the required energy for molecular mobility enlarges as the aging level deepens. Meanwhile, the D and Ea values of rejuvenators are remarkably higher and lower than that of aged binders, respectively. That's why all rejuvenators would effectively reactivate the molecular mobility and improve the stress relaxation performance of aged binders. However, the rejuvenation efficiency of Ea recovery is dependent on the rejuvenator type. The Ea values of naphthenic-oil and aromatic-oil rejuvenators are much larger than bio-oil and engine-oil, indicating that more energy is required for the molecular mobility of naphthenic-oil and aromatic-oil. The same finding is obtained based on the Log(τR)-(1/T) curves from relaxation tests.

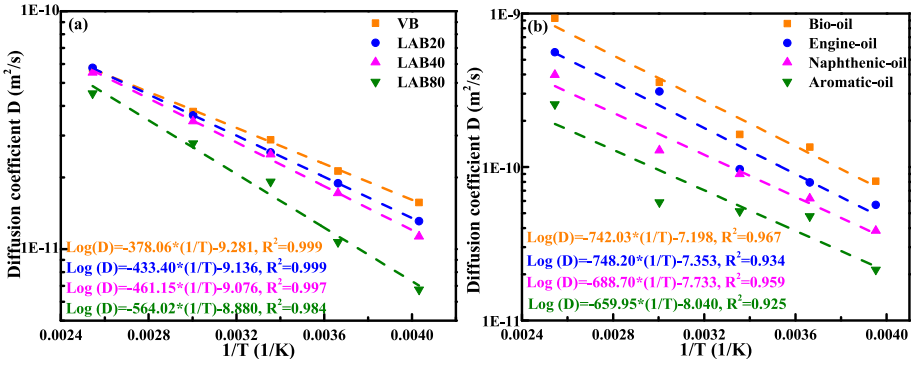

Fig. 24. Diffusion coefficient of aged bitumen and rejuvenators.

4.3. Volumetric parameters of aged bitumen and rejuvenators

Apart from the molecular characteristics, the relaxation behavior of bituminous material also depends on the amount of free volume in bitumen models. In other words, a large free volume creates a wide space environment for molecular motion and relaxation. It was also reported that the high free volume contributed to the low Tg value and relaxation time of polymer material (Patil et al., 2013). Therefore, the volumetric parameters (total, occupied, and free volume) of virgin/aged bitumen and rejuvenators are outputted and compared to explain the underlying reason for the difference in rejuvenation efficiency on relaxation performance of various rejuvenator-aged bitumen blends. The volumetric parameters of virgin/aged bitumen and rejuvenators are listed in Tables 16 and 17, respectively. The temperature varies from 253K to 393K to consider the temperature-susceptibility. It is observed that the temperature shows a significant influence on the total and free volume of bitumen and rejuvenator models, but it fails to affect the occupied volume dramatically. As temperature increases, molecular mobility and intermolecular distance are enhanced. Due to the difference in molecular structures and numbers in each bitumen and rejuvenator model, it is challenging to directly compare the difference in volumetric parameters considering the effect of aging level and rejuvenator type.

For quantitative comparison, the fractional free volume (FFV) is calculated as follows:

$$FFV = \frac{V - V_0}{V} \tag{11}$$

where FFV represents the fractional free volume, %; V and V_o are the total volume and occupied volume, $Å^3$.

Fig. 25 plots the FFV values of virgin/aged bitumen and rejuvenators at different temperatures. Irrespective of the simulation temperatures, the magnitude of FFV values of virgin/aged bitumen shows VB > LAB20 > LAB40 > LAB40. It means the free volume ratio of bitumen reduces significantly as the aging level rises, contributing to the increase in Tg value and reduction of the relaxation capacity of aged bitumen. In addition, all rejuvenators have higher FFV values than the aged binders, indicating that incorporating these rejuvenators can restore the free volume ratio of aged bitumen to a virgin bitumen level. Apart from the aging degree and rejuvenator dosage, the rejuvenator type may also show a distinct effect on the FFV value of rejuvenator-aged bitumen blends based on the difference in FFV values of different rejuvenators. The order of FFV values of the four rejuvenators is EO > BO > NO > AO, which is the same as the Tg ranking. It further validates that the Tg parameter is strongly attributed to the FFV index. Although the Tg and FFV parameters influence the relaxation performance of rejuvenated bitumen, it is insufficient to estimate the rejuvenation efficiency of rejuvenators on the relaxation behavior only with these two parameters, and the dominant role of molecular mobility parameter (diffusion coefficient) should be considered. In addition, the increment in temperature enlarges the FFV values of rejuvenators but has no impact on the ranking of FFV values for four rejuvenators. Thus, one temperature point is enough to compare the rejuvenation efficiency of rejuvenators on FFV value restoration of aged bitumen. However, the relationships between the temperature with the D and FFV parameters should be further investigated to determine the influence of temperature on the relaxation behaviors of rejuvenated binders.

Table 16
The volumetric parameters of virgin and aged bitumen.

Temperature	Rejuvenators	VB	LAB20	LAB40	LAB80
253K	Total ($Å^2$)	56679.94	57422.81	57377.49	58827.97
	Occupied ($Å^2$)	47305.08	48313.26	48844.31	49749.05
	Free ($Å^2$)	9374.86	9109.55	8533.18	9078.92
273K	Total ($Å^2$)	56978.44	57487.90	56864.54	58153.12
	Occupied ($Å^2$)	47345.97	47944.34	47385.97	48780.14
	Free ($Å^2$)	9632.47	9543.56	9029.36	9372.98
298K	Total ($Å^2$)	56564.12	57453.81	56757.82	58652.04
	Occupied ($Å^2$)	46753.15	47704.27	47953.83	48749.81
	Free ($Å^2$)	9810.97	9749.53	9371.85	9902.23
333K	Total ($Å^2$)	57641.05	58446.89	58066.60	59290.90
	Occupied ($Å^2$)	46886.28	47682.93	47922.99	48509.17
	Free ($Å^2$)	10754.77	10763.96	10143.61	10781.73
393K	Total ($Å^2$)	58625.40	59195.95	59652.34	60331.25
	Occupied ($Å^2$)	46581.21	47398.96	47549.87	48536.02
	Free ($Å^2$)	12044.19	11796.99	12102.47	11795.23

5. Conclusions and recommendations

This study aims to investigate the coupling effects of rejuvenator type/dosage and aging degree of bitumen on the relaxation behaviors and propose the critical indicators for evaluating the rejuvenation efficiency on low-temperature relaxation performance of rejuvenated bitumen. The main conclusions and recommendations are shown below:

5.1. Main conclusions

(1) Long-term aging increases shear stress τ, relaxation time t, and residue stress ratio R values of bitumen, tending to decrease after adding rejuvenators. The τ and t values of rejuvenated bitumen show a linear relationship with rejuvenator dosage, while the R value enlarges exponentially. The bio-oil rejuvenator exhibits the highest rejuvenation efficiency, followed by the engine-oil and naphthenic-oil, while the aromatic-oil shows the lowest effectiveness.

(2) The proposed relaxation model can describe the relaxation curves of rejuvenated binders. The model parameter A decreases, and n increases with the rejuvenator dosage increment. The magnitude of AR values for rejuvenated bitumen is BORB > EORB > NORB > AORB, but the order of nR values is not constant relying on the rejuvenator dosage and aging degree of bitumen.

(3) All relaxation parameters of aged bitumen are regenerated by adding rejuvenators. The rejuvenation effectiveness of various rejuvenators can be distinguished with the relaxation model parameter A but not by parameter n. Moreover, the parameters τ_{50s}, $t_{25\%}$, and A are recommended as critical indicators for evaluating the rejuvenation efficiency on relaxation performance of different rejuvenator-aged bitumen blends.

(4) The molecular mobility and free volume ratio of rejuvenators mainly cause the difference in the rejuvenation efficiency of various rejuvenators on the relaxation property. The diffusion capacity of rejuvenators exhibits a more dominant effect on rejuvenation efficiency than fractional free volume.

5.2. Recommendations for future work

(1) Further validation of the proposed critical indicators is necessary for other rejuvenator-aged bitumen blends, including those with different rejuvenators such as Tall-oils. Additionally, it is crucial to explore the correlation between these essential relaxation indices of rejuvenated bitumen and the low-temperature properties of recycled asphalt mixtures.

(2) We will conduct molecular dynamics (MD) simulations on various rejuvenated bitumen and output their thermodynamic properties, such as Tg, D, and FFV, which will then be correlated with the critical relaxation indicators of τ_{50s}, $t_{25\%}$, and A.

Table 17
The volumetric parameters of four rejuvenators at different temperatures.

Temperature	Rejuvenators	BO	EO	NO	AO
253K	Total (Å^2)	110296.65	121834.77	133027.99	136060.43
	Occupied (Å^2)	92830.48	100311.92	110377.18	113457.33
	Free (Å^2)	17466.17	21522.85	22650.81	22603.10
273K	Total (Å^2)	112209.10	123210.60	133824.37	136510
	Occupied (Å^2)	92337.26	100050.59	110349.39	113553.74
	Free (Å^2)	19871.83	23160.02	23474.98	22956.26
298K	Total (Å^2)	113148.08	124563.97	135111.31	137110.56
	Occupied (Å^2)	92166.95	99271.31	110092.21	113698.67
	Free (Å^2)	20981.13	25292.66	25019.10	23411.99
333K	Total (Å^2)	117206.99	127777.74	137943.30	139434.71
	Occupied (Å^2)	91169.90	99057.06	109496.56	113312.19
	Free (Å^2)	26037.09	28720.68	28446.74	26122.52
393K	Total (Å^2)	122374.82	133917.26	143878.00	144287.97
	Occupied (Å^2)	89880.39	97549.88	108169.93	112290.13
	Free (Å^2)	32494.42	36367.38	35708.07	31997.85

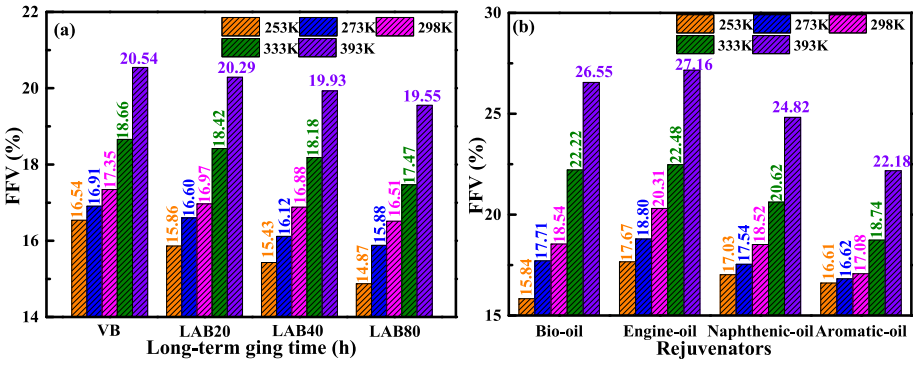

Fig. 25. The fractional free volume (FFV) of virgin/aged binders and rejuvenators.

CRediT authorship contribution statement

Shisong Ren: Methodology, Investigation, Simulation, Formal analysis, Writing – original draft, Writing – review & editing. **Xueyan Liu:** Supervision, Writing – review & editing. **Sandra Erkens:** Methodology, Supervision.

Declaration of competing interest

The authors declare that they have no known competing financial interests or personal relationships that could have appeared to influence the work reported in this paper.

Data availability

Data will be made available on request.

Acknowledgments

The first author would thank the funding support from the China Scholarship Council (CSC, No.201906450025).

Appendix A. Supplementary data

Supplementary data to this article can be found online at https://doi.org/10.1016/j.jclepro.2023.139092.

References

Ahmed, R., Hossain, K., 2020. Waste cooking oil as an asphalt rejuvenator: a state-of-the-art review. Construct. Build. Mater. 230, 116985.
Bai, M., 2017. Investigation of low-temperature properties of recycling of aged SBS modified asphalt binder. Construct. Build. Mater. 150, 766–773.
Behnood, A., 2019. Application of rejuvenators to improve the rheological and mechanical properties of asphalt binders and mixtures: a review. J. Clean. Prod. 231, 171–182.
Buchner, J., Wistuba, M., Miesem, S., Neliepp, M., Dietzsch, M., Sandor, M., 2023a. Rheological characterisation of rejuvenator blending lines. Road Mater. Pavement Des., 2180994
Buchner, J., Rys, D., Trifunovic, S., Wistuba, M., 2023b. Development and application of asphalt binder relaxation test in different dynamic shear rheometers. Construct. Build. Mater. 364, 129929.
Deng, M., Cao, X., Li, Z., Li, X., Yang, X., Tang, B., 2022. Investigating properties and intermolecular interactions of sludge bio-oil modified asphalt. J. Mol. Liq. 360, 119415.
Fang, Y., Zhang, Z., Yang, J., Li, X., 2021. Comprehensive review on the application of bio-rejuvenator in the regeneration of waste asphalt materials. Construct. Build. Mater. 295, 123631.
Fu, Q., Xie, Y., Niu, D., Long, G., Luo, D., Yuan, Q., Song, H., 2016. Integrated experimental measurement and computational analysis of relaxation behavior of cement and asphalt mortar. Construct. Build. Mater. 120, 137–146.
Gulzar, S., Fried, A., Preciado, J., Castorena, C., Underwood, S., Habbouche, J., Boz, I., 2023. Towards sustainable roads: state-of-the-art review on the use of recycling agents in recycled asphalt mixtures. J. Clean. Prod., 136994
Hofer, K., Mirwald, J., Bhasin, A., Hofko, B., 2023. Low-temperature characterization of bitumen and correlation to chemical properties. Construct. Build. Mater. 366, 130202.
Jing, R., Varveri, A., Liu, X., Scarpas, A., Erkens, Rheological, S., 2020. Fatigue and relaxation properties of aged bitumen. Int. J. Pavement Eng. 21 (8), 1024–1033.
Jing, R., Varveri, A., Liu, X., Scarpas, A., Erkens, S., 2021. Differences in the ageing behavior of asphalt pavements with porous and stone mastic asphalt mixtures. Transport. Res. Rec. 2675 (12), 1138–1149.
Kumbargeri, Y., Planche, J., Adams, J., Elwardany, M., King, G., 2023. Effect of binder chemistry and related properties on the low-temperature performance parameters of asphalt binders. Transport. Res. Rec. 1–19.
Li, F., Wang, Y., Miljkovic, M., Chan, K., 2022. Changes in the nanoscale asphaltene particles and relaxation spectra of asphalt binders during aging and rejuvenation. Mater. Des. 219, 110808.
Lin, P., Liu, X., Apostolidis, P., Erkens, S., Ren, S., Xu, S., Scarpas, T., Huang, W., 2021. On the rejuvenator dosage optimization for aged SBS modified bitumen. Construct. Build. Mater. 271, 121913.
Liu, C., Du, J., Wu, C., Liu, K., Jiang, K., 2022. Low-temperature crack resistance of wood tar-based rejuvenated asphalt based on viscoelastic rheological method. Int. J. Pavement Res. Technol. 15, 1340–1353.

Liu, S., Qi, X., Shan, L., 2022. Effect of molecular structure on low-temperature properties of bitumen based on molecular dynamics. Construct. Build. Mater. 319, 126029.
Luo, L., Liu, P., Leischner, S., Oeser, M., 2023. Atomic insights into the nano-cracking behaviour of bitumen: considering oxidative aging effects. Road Mater. Pavement Des., 2180292
Mansourkhaki, A., Ameri, M., Habibpour, M., Underwood, B., 2020. Relations between colloidal indices and low-temperature properties of reclaimed binder modified with softer binder, oil-rejuvenator and polybutadiene rubber. Construct. Build. Mater. 239, 117800.
Mokhtari, A., Lee, H., Williams, R., Guymon, C., Scholte, J., Schram, S., 2017. A novel approach to evaluate fracture surfaces of aged and rejuvenator-restored asphalt using cyro-SEM and image analysis techniques. Construct. Build. Mater. 133, 301–313.
Ncat, 2014. NCAT Researchers Explore Multiple User of Rejuvenators Asphalt Technology News, vol. 26, pp. 1–16, 1.
Pang, L., Liu, K., Wu, S., Lei, M., Chen, Z., 2014. Effect of LDHs on the aging resistance of crumb rubber modified asphalt. Construct. Build. Mater. 67, 239–243.
Patil, P., Rath, S., Sharma, S., Sudarshan, K., Maheshwari, P., Patri, M., Praveen, S., Khandelwal, P., Pujari, P., 2013. Free volumes and structural relaxations in diglycidyl ether of bisphenol-a based epoxy-polyether amine networks. Soft Matter 9, 3589.
Pei, Z., Yi, J., Xu, M., Ai, X., Cao, J., Hu, W., Gao, L., Feng, D., 2023. Exploration of the design theory of crack-resistance rejuvenator for warm-mix recycled asphalt mixtures with high RAP contents. J. Clean. Prod. 388, 135855.
Rajib, A., Samieadel, A., Zalghout, A., Kaloush, K., Sharma, B., Fini, E., 2022. Do all rejuvenators improve asphalt performance? Road Mater. Pavement Des. 23 (2), 358–376.
Ren, M., Li, Y., Cheng, P., Chen, Y., 2022. Effect of modifier on low-temperature reversible aging behavior of asphalt binder and its morphology analysis. Construct. Build. Mater. 351, 128943.
Ren, S., Liu, X., Fan, W., Qian, C., Nan, G., Erkens, S., 2021a. Investigating the effects of waste oil and styrene-butadiene rubber on restoring and improving the viscoelastic, compatibility, and aging properties of aged asphalt. Construct. Build. Mater. 269, 121338.
Ren, S., Liu, X., Lin, P., Erkens, S., Xiao, Y., 2021b. Chemo-physical characterization and molecular dynamics simulation of long-term aging behaviors of bitumen. Construct. Build. Mater. 302, 124437.
Ren, S., Liu, X., Lin, P., Erkens, S., Gao, Y., 2022. Chemical characterizations and molecular dynamics simulations on different rejuvenators for aged bitumen recycling. Fuel 324, 124550.
Schwettmann, K., Nytus, N., Weigel, S., Radenberg, M., Stephan, D., 2023. Effects of rejuvenators on bitumen ageing during simulated cyclic reuse: a review. Resour. Conserv. Recycl. 190, 106776.
Shi, K., Ma, F., Liu, J., Song, R., Fu, Z., Dai, J., Li, C., Wen, Y., 2022. Development of a new rejuvenator for aged SBS modified asphalt binder. J. Clean. Prod. 380, 134986.
Sonibare, K., Rucker, G., Zhang, L., 2021. Molecular dynamics simulation on vegetable oil modified model asphalt. Construct. Build. Mater. 270, 121687.
Sun, D., Sun, G., Zhu, X., Ye, F., Xu, J., 2018. Intrinsic temperature sensitive self-healing character of asphalt binders based on molecular dynamics simulations. Fuel 211, 609–620.
Sun, W., Wang, H., 2022. Molecular dynamics simulation of nano-crack formation in asphalt binder with different SARA fractions. Mol. Simulat. 48 (9), 789–800.
Wang, D., Falchetto, A., Riccardi, C., Westerhoff, J., Wistuba, M., 2021. Investigation on the effect of physical hardening and aging temperature on low-temperature rheological properties of asphalt binder. Road Mater. Pavement Des. 22 (5), 1117–1139.
Wang, J., Lv, S., Liu, J., Peng, X., Lu, W., Wang, Z., Xie, N., 2023. Performance evaluation of aged asphalt rejuvenated with various bio-oils based on rheological property index. J. Clean. Prod. 385, 135593.
Wang, T., Wang, J., Hou, X., Xiao, F., 2021. Effects of SARA fractions on low temperature properties of asphalt binders. Road Mater. Pavement Des. 22 (3), 539–556.
Xing, B., Fan, W., Lyu, Y., Che, J., Zhuang, C., 2020. Influences of ball-milled limestone particle sizes and shapes on asphalt mastic stress relaxation behavior. Construct. Build. Mater. 255, 119396.
Xu, J., Fan, Z., Lin, J., Yang, X., Wang, D., Oeser, M., 2021a. Predicting the low-temperature performance of asphalt binder based on rheological model. Construct. Build. Mater. 302, 124401.
Xu, J., Fan, Z., Lin, J., Liu, P., Wang, D., Oeser, M., 2021b. Study on the effects of reversible aging on the low temperature performance of asphalt binders. Construct. Build. Mater. 295, 123604.
Yan, K., Lan, H., Duan, Z., Liu, W., You, L., Wu, S., Miljkovic, M., 2021. Mechanical performance of asphalt rejuvenated with various vegetable oils. Construct. Build. Mater. 293, 123485.
Yao, H., Liu, J., Xu, M., Jie, J., Dai, Q., You, Z., 2022. Discussion on molecular dynamics (MD) simulations of the asphalt materials. Adv. Colloid Interface Sci. 299, 102565.
Yaphary, Y., Leng, Z., Wang, H., Ren, S., Lu, G., 2022. Characterization of nanoscale cracking at the interface between virgin and aged asphalt binders based on molecular dynamics simulations. Construct. Build. Mater. 335, 127475.
Zeng, Z., Underwood, B., Castorena, C., 2022. Low-temperature performance grade characterisation of asphalt binder using the dynamic shear rheometer. Int. J. Pavement Eng. 23 (3), 811–823.
Zhang, L., Hussain, B., Tan, Y., 2015. Effect of bio-based and refined waste oil modifiers on low temperature performance of asphalt binders. Construct. Build. Mater. 86, 95–100.
Zhang, L., Greenfield, M., 2007. Relaxation time, diffusion, and viscosity analysis of model asphalt systems using molecular simulation. J. Chem. Phys. 127, 194502.
Zhao, K., Wang, Y., Chen, L., Li, F., 2018. Diluting or dissolving? The use of relaxation spectrum to assess rejuvenation effects in asphalt recycling. Construct. Build. Mater. 188, 143–152.
Zheng, W., Yang, Y., Chen, Y., Yu, Y., Hossiney, N., Tebaldi, G., 2022. Low temperature performance evaluation of asphalt binders and mastics based on relaxation characteristics. Mater. Struct. 55, 204.